

THESIS FOR THE DEGREE OF LICENTIATE OF ENGINEERING

**Nitride fuel production by the internal sol gel process**

MARCUS HEDBERG



Nuclear Chemistry

Department of Chemical and Biological Engineering

CHALMERS UNIVERSITY OF TECHNOLOGY

Gothenburg, Sweden 2014

Nitride fuel production by the internal sol gel process

© MARCUS HEDBERG, 2014

Technical report no 2014:12

ISSN nr: 1652-943X.

Nuclear Chemistry

Department of Chemical and Biological Engineering

Chalmers University of Technology

SE – 412 96 Göteborg

Sweden

Telephone +46(0)31-772 1000

Cover:

SEM image of microspheres produced by the internal sol gel technique.

Chalmers Reproservice

Gothenburg, Sweden 2014

# Nitride fuel production by the internal sol gel process

Marcus Hedberg

Nuclear Chemistry

Department of Chemical and Biological Engineering

Chalmers University of Technology

## Abstract

During operation of a fourth generation reactor system it is necessarily not desirable to utilize an oxide fuel matrix as in light water reactor systems. One type of chemical compounds that has been suggested is nitride based nuclear fuel. Nitride fuels possess several characteristics that make them interesting for reactor operation such as high melting point, high thermal conductivity and better chemical compatibility compared to oxides with liquid metal coolants such as sodium or lead. Nitride fuel can be produced either as pure actinide nitride fuel such as UN or as fuel where the fissile material is diluted in an inert matrix such as (Zr, Pu)N. A problem with nitride fuel is the production process. Nitrides are not stable in air and production must thus be performed under inert atmosphere to reduce oxygen uptake in the material. Also residual oxygen and carbon content from production and processing is an issue that needs to be addressed. Spontaneous oxidation in air together with radiological safety concern regarding handling fine powders of actinide nitrides such as PuN for example provides an incitement for evaluating potential dust free processes for nitride fuel production. Work has been performed on production of ZrN as an inert fuel matrix by the internal sol gel process and subsequent carbothermal reduction. Elemental carbon suspension sols have been produced and gelled into microspheres. Heat treatments of the produced microspheres in N<sub>2</sub> + 5 % H<sub>2</sub> gas mixture was performed during nitridation. Elemental investigation of the produced microspheres suggested an approximate composition of Zr(N<sub>0.7-0.8</sub>C<sub>0.2-0.3</sub>). Pelletization of the nitride microspheres produced pellets with blackberry structure and XRD measurements on sintered material also suggested a material composition of about Zr(N<sub>0.8</sub>C<sub>0.2</sub>).

**Keywords:** Nitride, ZrN, internal sol gel, carbothermal reduction, sintering



# Table of contents

<b>1. Introduction .....</b>	<b>1</b>
<b>2. Background.....</b>	<b>3</b>
2.1. Thermal neutron reactors .....	4
2.2. Fast neutron reactors .....	5
2.3. Nuclear fuel .....	6
2.3.1. Oxide nuclear fuel.....	7
2.3.2. Nitride nuclear fuel .....	7
2.3.3. Carbide nuclear fuel.....	8
2.4. Fuel types and geometries .....	9
2.5. Introduction to sol gel techniques for nuclear fuel production .....	9
<b>3. Theory .....</b>	<b>11</b>
3.1. Nitrides as a nuclear fuel ceramic .....	11
3.1.1. Thermal conductivity of nitrides.....	11
3.1.2. Melting temperature.....	11
3.1.3. Drawbacks of nitrides .....	12
3.1.4. Nitride production techniques.....	13
3.2. Internal sol gel .....	14
3.3. Dispersion agents and carbon dispersions.....	16
3.4. Carbothermal reduction.....	16
3.5. Pelletization and sintering .....	19
3.5.1. Pelletization .....	19
3.5.2. Sintering.....	19
3.6. Characterization .....	21
3.6.1. Scanning Electron Microscopy and Energy dispersive X-ray Spectroscopy.....	21
3.6.2. SEM/EDX measurements .....	22

3.6.3. X-ray diffraction .....	22
3.6.4. XRD measurements .....	23
3.6.5. Analytical methods for light element quantification .....	24
<b>4. Experimental procedures .....</b>	<b>25</b>
4.1. Preparation of zirconium sols.....	25
4.2. Water migration to the silicone oil.....	26
4.3. Preparation of uranium containing sols.....	27
4.4. Nitridation of zirconium microspheres .....	27
4.5. Pressing of ZrN and sintering.....	29
<b>5. Results and discussion.....</b>	<b>31</b>
5.1. Carbon stabilization by addition of dispersion agent.....	31
5.2. Water leakage into silicone oil .....	32
5.3. Gelation of zirconium containing microspheres .....	33
5.3.1. Effect of nozzle vibration .....	33
5.3.2. Effects of carbon addition to the sol .....	35
5.4. Gelation of uranium containing microspheres .....	36
5.5. Nitriding of zirconium containing microspheres .....	39
5.6. Sintering of pellets .....	41
<b>6. Conclusions .....</b>	<b>49</b>
<b>7. Future work .....</b>	<b>51</b>
<b>8. Acknowledgements.....</b>	<b>53</b>
<b>9. Bibliography .....</b>	<b>55</b>
<b>10. List of abbreviations.....</b>	<b>61</b>

## Appendix I

# 1. Introduction

Energy is vital in modern society. The use of electricity simplifies the lives of humans and today is so integrated into society that it is almost impossible to live without it. In short, electricity is a highly desirable product that few people if any are really willing to do without. The electricity must, however, be produced by some means and different production techniques are associated with differing environmental impact and production cost. Today most people agree that CO<sub>2</sub> emissions from electricity production ought to be reduced to combat unwanted climate change. In electricity terms this means that in order for us to carry on consuming electricity the CO<sub>2</sub>-emitting technologies common in electricity production today, such as burning of oil and coal, need to be reduced. One technology that can contribute to lower CO<sub>2</sub> emissions in the electricity sector is nuclear power.

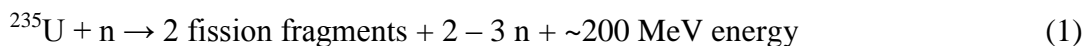
Electric production capacity in the world originating from commercial nuclear power totaled 372.1 GW(e) shared between 437 reactors at the end of 2012 [IAE 13]. As of January 2013 there were also 247 research reactors in operation worldwide. In Sweden, with its 10 operating nuclear reactors, the nuclear sector of the power-generating industry provided 9 395 MW(e) in 2012. In total that represented 38.1 % of electricity produced in Sweden [IAE 13].

Two main drawbacks commonly associated with the use of nuclear energy are the risk of accidents and release of artificial radioactivity into the environment and the waste remaining once the fuel has been used. After the accident at Fukushima in 2011 there has been renewed discussion of the level of safety in nuclear power, and Germany has decided to decommission all its nuclear power. The basis of nuclear energy development is thus still, as it has been throughout the nuclear era, continuous development of safer reactors and ability to extract as much energy as possible from the fuel used in order to minimize the waste fraction. One important parameter affecting nuclear power safety and fuel utilization and behavior in-pile and during potential reprocessing is the chemical form of the fuel used. This thesis focuses on the production and characterization of ZrN as an inert matrix material produced by the internal sol gel technique and subsequent carbothermal reduction.



## 2. Background

A nuclear reactor is essentially a water boiler. The aim of a nuclear power plant is to produce electricity, and the means by which this is done is production of steam that can drive turbines and generators that produce the desired electricity. In this respect a nuclear power plant differs little from a plant that generates electricity by burning material such as coal, oil or biomass, for instance. The way to electricity in all these cases is through steam. What makes a nuclear power plant different from traditional combustion-based techniques is the origin of the energy. In all forms of energy extraction involving combustion, the energy released originates from the forces that bind atoms together into molecules, the chemical bonds. In nuclear power production the energy does not originate from inter-atomic forces but from the atomic nuclei themselves. Neutron irradiation may cause heavy nuclei to fission. During fission the nucleus splits into two smaller nuclei and at the same time additional neutrons and energy are released. The energy released during a fission reaction is about 200MeV [CHO 02]. Using  $^{235}\text{U}$  as an example, the overall fission reaction thus becomes



This is to be compared to conventional combustion where the energy released per reaction is of the order of a couple of eV. Nuclear power is thus an extremely energy-dense technology compared to other means of extracting energy.

Nuclear reactors come in various shapes and sizes. Over the years since the dawn of nuclear reactors several different reactor concepts have been developed. Sometimes the term generations is used as an overview of emerging reactors during nuclear power evolution. The first generation of reactors, developed in the 1950s and 1960s, was that of metal-fueled prototype reactors. The second generation of reactors was the first reactor fleet of commercial power producing reactors, introducing amongst others light-water reactors such as the Boiling Water Reactor (BWR) and the Pressurized Water Reactor (PWR). Reactors built today and over the past few years belong to the third generation of nuclear reactors and mainly comprise what are known as Advanced Light Water Reactors, which is a development of the second reactor generation. There is an ad hoc enhancement of the generation III reactor concept that may make up the next wave of reactors, the generation III+ group. Generation III+ are conceptually generation III reactors but are refined and further developed. A feature common to all reactor generations discussed so far is that they operate using thermal neutrons and utilize  $^{235}\text{U}$  as the fissile part of the fuel.

As well as the reactors discussed so far there is another group of nuclear reactors. A group that has been around since the 1950s but not reached a commercial power-producing level and that is the fast neutron reactors. These types of reactors are potentially able to use the nuclear fuel much more efficiently than the commercial reactors of today. Fast neutron reactors can also be designed as breeder reactors. This means that fast neutron reactors can produce more fissile material from neutron capture in  $^{238}\text{U}$  than they consume during operation. This would

allow much more effective use of the fuel compared to commercial reactors used today. Fast neutron reactors would also be able to use actinides higher up in the periodic table than uranium as fuel. Since such actinides are being net produced in present-day reactors it would be possible to use what today is considered to be waste as a future fuel.

To be able to utilize present-day nuclear waste as novel nuclear fuels there is a need to be able to recycle the desired actinides from the used fuel. This means that the more or less open once-through fuel cycle used in nuclear power today has to be closed. This implies that a fourth generation of nuclear energy should not be thought of as merely a reactor concept but rather as an entire system including separation and re-fabrication of nuclear fuel in the process. The actinides desired for recycling in a generation IV system cause a significant increase in radioactivity and dose rate during separation and fuel re-fabrication. Therefore new methods for fuel production need to be investigated in order to develop the safest fuel-handling process possible. A fast reactor fleet would also mean that different requirements have to be met by the materials used in the reactors compared to earlier reactor generations. For potential commercialization of fast neutron reactors it is thus necessary to investigate and develop novel types of materials as cladding materials, core coolants and, last but not least, new chemical compositions of the nuclear fuel. Figure 1 illustrates the development of different reactor generations.

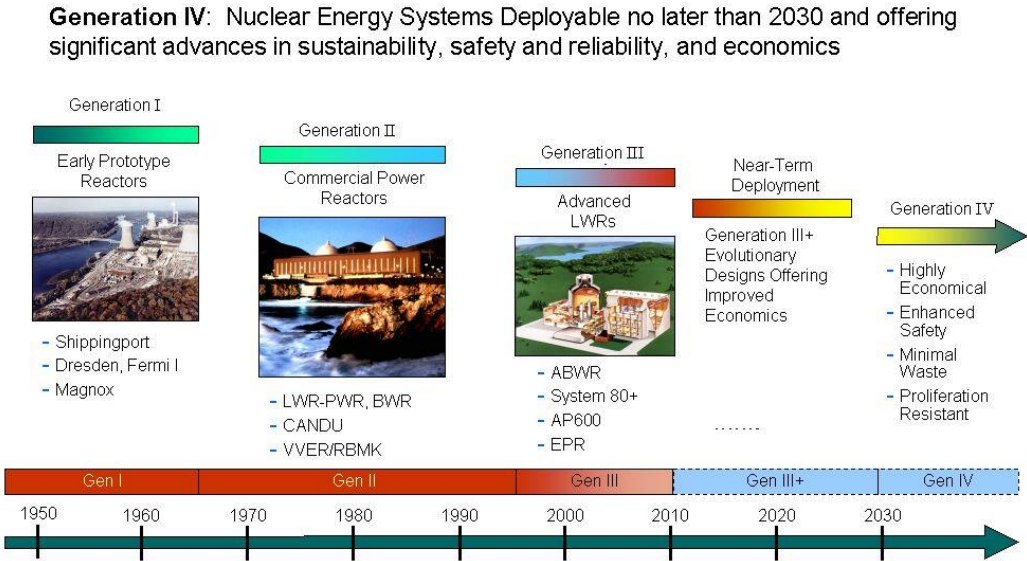


**Figure 1.** Schematic illustration of the development and predicted evolution of nuclear reactor generations.

### 2.1. Thermal nuclear reactors

The vast majority of commercial nuclear power production at present is based on moderated water cooled reactors [IAE 13]. In a moderated reactor the highly energetic neutrons emitted by fission are slowed down, also called thermalized, to what is called the thermal energy region [CHO 02]. A neutron that is thermal possesses energy in the region of  $K_B T$ , where  $K_B$  is Boltzmann’s constant and T is the absolute temperature measured in Kelvin, and the kinetic

energy of a thermalized neutron is about 0.025 eV. The reason for wanting to thermalize the neutron flux in a nuclear reactor is that the reactivity of the neutrons or probability of interaction with atomic nuclei, if one wishes, is highly dependent on the energy of the neutrons. The moderator may shift for example between graphite, light water and heavy water. When water is used as moderator it is simultaneously utilized as a heat carrier, removing the heat produced by the core to the electricity-producing turbines. When graphite is used as a moderator the heat is removed by using flow channels through the core and the heat-carrying medium is either water or gas. Thermalization of the neutrons occurs by elastic scattering reactions with low-weight atoms such as hydrogen or carbon, where energy is transferred to the atom nucleus upon impact. This can be visualized as being like when a moving cue ball hits a stationary one: after the collision the kinetic energy will have divided between the two balls and the initially moving one will have slowed down somewhat. When the nucleus becomes heavier, on the other hand, very little energy is transferred to the nucleus in the scattering reaction. This can be more compared to when a tennis ball hits a brick wall. The tennis ball will rebound at about the same speed as its incoming speed while the brick wall will be stationary.

## 2.2. Fast neutron reactors

A reactor which does not operate with neutrons in the thermal energy region but instead is run directly using the high-energy neutrons emitted by fission is said to be a fast neutron reactor. The probability of a neutron inducing fission in a fissile atom such as  $^{235}\text{U}$  or  $^{239}\text{Pu}$  is lower for high-energy neutrons than thermal ones. However, a high-energy neutron spectrum has the advantage of being able to effectively use a larger number of actinide nuclei as nuclear fuel. The nuclei that can be utilized as fuel in a high-energy spectrum include additional plutonium isotopes and also isotopes of americium and curium. This makes fast-neutron reactors a candidate solution for transmutation of minor actinides produced in commercial power reactors, producing additional electricity in the process. Since moderation of neutrons is unwanted in fast reactors, water is not used as the core coolant and other coolants such as pressurized gas and liquid metals, for example sodium or lead, are favored instead. The use of such coolants also leads to improved neutron economy compared to moderated reactors where the thermal neutrons are to a larger degree consumed by neutron capture reactions in moderator, coolant and structure materials. The fast reactor concept is not new, and the first reactor of this kind was the EBR I, started as long ago as 1951 [MAT 86]. The fast reactors never really reached commercialization, however, the light-water moderated reactor in particular becoming the reactor type chosen instead. So far the fast neutron reactors have mostly remained at the research stage and as prototype reactors in the civil sector and in the military as propulsion systems for submarines [BLA 88, WAL 12].

Another feature of the fission induced in the fast neutron spectrum is that the average number of new neutrons emitted during a fission reaction will be somewhat higher than when using a thermal neutron spectrum. In all nuclear reactors new fissile material can be produced by neutron capture in fertile atoms such as production of  $^{239}\text{Pu}$  by neutron capture and

subsequent  $\beta^-$  decay in  $^{238}\text{U}$ . A thermal reactor is basically a consumer of fuel since it uses more fuel during operation than it produces, however when a fast reactor is used it is possible, due to the higher neutron yield and improved neutron economy, to construct a reactor that produces more fuel than it consumes during operation. These kinds of reactors are commonly referred to as breeder reactors, and breeder reactors using liquid metal as coolant have come to form their own category of nuclear reactors known as Liquid Metal Fast Breeder Reactors (LMFBR) [MAT 91]. The fast reactor concept is not explicitly dedicated to breeding purposes, however. A fast reactor can also be utilized for burning actinides without breeding if using plutonium based fuels, for example, with no  $^{238}\text{U}$  mixed in or utilized as blanket material [ROG 11].

The smaller reaction cross-section of fast neutrons compared to thermal neutrons results in a fast neutron reactor operating at a higher neutron flux compared to a moderated reactor. The higher neutron flux will affect the materials in the reactor by dislocating atoms in the lattice structures. The average number of times an atom is moved within its structure during in-core operation is normally expressed as dislocations per atom (DPA). This increases the demands for durability of the materials used in the core such as the cladding material and the fuel itself, since the number of times on average that the atoms in the materials will move in their respective structures will increase from about 1 DPA / year to about 40 DPA / year [WAL 11].

### **2.3. Nuclear fuel**

To be a suitable nuclear fuel, there are several properties that have to be fulfilled. Some are reactor system specific such as the ability to be compatible with the cladding material used in the case of pellet cladding mechanical interaction (PCMI) and displaying chemical resistance to the coolant used in the system. Other desired properties are more general such as high heat capacity and thermal conductivity. The heat capacity affects how quickly the core responds to some transient behaviors. This is because temperature increase in the system is coupled to the neutron flux profile and reactivity in the core. The thermal conductivity governs how rapidly heat can be transported from the core to the coolant and will affect the operational temperature of the fuel during in-pile performance. A fuel with higher thermal conductivity will allow for a lower operational temperature in the fuel. This will allow for a larger margin to the melting point of the fuel and increase the safety features of the reactor.

One important property of a nuclear fuel material is its melting temperature. A high melting temperature is advantageous in order to keep the margin between operational temperature and melting temperature wide. For example if using a metallic fuel the heat conductivity will be high and thus the in-pile temperature can be kept relatively low. However, the melting temperature of metallic fuel is quite low. Ceramic oxide fuels, on the other hand, have a lower thermal conductivity and higher operation temperature. The melting point of oxides is much higher than for metals, so the residual temperature gap between operational temperature and melting temperature may still be wider for oxides than for metals.

There are several different types of chemical compounds that can be utilized as nuclear fuel. Nuclear fuels can be divided into two main categories, metallic and ceramic. Within the ceramic category there are several different types of fuel such as oxides, nitrides and carbides.

### **2.3.1. Oxide nuclear fuel**

Oxide-based nuclear fuel is the most common fuel type used both today and historically. Normally the oxide fuel used in nuclear reactors is  $\text{UO}_2$  but there is also mixed oxide fuel (MOX), which consists of  $(\text{U,Pu})\text{O}_2$ . Reasons why the oxide form is the most common fuel type used include the fact that it is easier to fabricate compared to carbide or nitride fuels. Oxide fuels generally also have good high-temperature stability, high melting point and good chemical compatibility towards water, which is a very common core moderator and coolant. Today there is also a considerable experience base of operating oxide fuels since it is basically the chemical fuel form utilized in most power producing reactors worldwide [BLA 89].

### **2.3.2. Nitride nuclear fuel**

Nitride-based nuclear fuel has several characteristics that makes it an interesting chemical composition for nuclear fuel purposes. The nitride chemical forms of uranium and plutonium, for example, have a higher density than their oxide counterparts. The thermal conductivity is far higher than that of the oxides, while the melt temperature is approximately equally high. A summarizing comparative table of uranium and plutonium properties in their nitride respectively oxide form is presented as Table 1.

**Table 1.** Illustration of the heat capacity, theoretical density, thermal conductivity and melt temperature for the nitride and dioxide chemical compounds of uranium and plutonium.

Property	UO <sub>2</sub>	PuO <sub>2</sub>	UN	PuN
Heat capacity (1000 °C) (J·mol·K <sup>-1</sup> )	~86 [POP 00]	~92 [POP 00]	~ 63 [HAY 90, OET 72]	~65 [OET 78]
Heat capacity (1500 °C) (J·mol·K <sup>-1</sup> )	~94 [POP 00]	~102 [VÄL 14]	~ 68 [HAY 90, OET 72]	~68 [KUR 00]**
Heat capacity (2000 °C) (J·mol·K <sup>-1</sup> )	~116 [POP 00]		~75 [HAY 90a, OET 72]	~72 [KUR 00]**
Theoretical density (g·cm <sup>-3</sup> )	10.97 [HAY 12]	11.5 [HAY 12]	14.33 [HAY 90b]	14.4 [HAY 12]
Crystal structure	FCC – CaF <sub>2</sub> type [ALL 67]	FCC – CaF <sub>2</sub> type [BEG 90]	FCC – NaCl type [ALL 67]	FCC – NaCl type [GAN 97]
Melt temperature (°C)	2847 [HAY 12]	2428 [ADA 85]	2780 decomposition under 1 bar N <sub>2</sub> [OLS 63]	2570 decomposition under 1 bar N <sub>2</sub> [OET 67]
Thermal conductivity (1000 °C) (W·K <sup>-1</sup> ·m <sup>-1</sup> )	~2.8 [POP 00]*	~3 [GIB 71]	~25 [KLE 99]	~11 [ARA 98]
Thermal conductivity (1500 °C) (W·K <sup>-1</sup> ·m <sup>-1</sup> )	~2.1 [POP 00]*	~2.2 [GIB 71]	~27 [KLE 99]	
Thermal conductivity (2000 °C) (W·K <sup>-1</sup> ·m <sup>-1</sup> )	~2.1 [POP 00]*		~28 [KLE 99]	

\*Data applicable to material with 95 % Theoretical Density (TD).

\*\* Data predicted by molecular dynamics simulations.

Several of the property values presented in Table 1 are by no means constant but change with temperature. In order to illustrate the differences between oxide and nitride properties, parameter values are presented at chosen temperatures. This is done to demonstrate the qualitative difference between nitride and oxide fuel. Therefore a few selected temperatures over a wide temperature region are selected instead of full graphs describing parameter properties.

### 2.3.3. Carbide nuclear fuel

Carbides are chemical compounds that like nitrides are being considered as a potential candidate for usage as nuclear fuel. The actinide carbides share several similarities with the

nitrides, such as high thermal conductivity. Both actinide nitrides and carbides of, for example, americium also display degradation and volatilization during production and sintering at high temperatures, and this behavior is more pronounced in the carbide than nitride [WAL 11]. As a general comparison, nitrides have somewhat higher melt temperature and metal density [SOM 11, BEN 69]. In powder state the actinide carbides display pyrophoric characteristics in air. This is, however, a property also shared by fine powders of actinide nitrides. Compared to nitrides, carbides possess better neutron economy during in-pile operation due to lower production of  $^{14}\text{C}$ . This also makes carbides easier to fabricate in the sense that nitrides require the use of  $^{15}\text{N}$  in order to lower  $^{14}\text{C}$  production by (n, p) reaction on  $^{14}\text{N}$  during in-pile operation [MAT 86]. Carbides as a nuclear fuel material constitute a research field of their own and will not be covered as a nuclear fuel material within this thesis but only as an undesired residue solution in produced nitride fuels.

## 2.4. Fuel types and geometries

The most common physical form of nuclear fuel used in power generating reactors is the fuel pellet. A fuel pellet is cylindrically shaped and has height and diameter both of roughly 10 mm, although some variations in physical dimensions do occur. A nuclear fuel core is made up of fuel assemblies, each of which constitutes a separate movable unit which is loaded into the reactor core during fuel exchange. Every fuel assembly in turn is made up of fuel pins. The fuel pins are hollow tubes in which the nuclear fuel pellets are stacked on top of each other.

There are, however, different ways of filling a fuel pin, apart from stacking pellets. One possibility would be to produce small spheres in a size range of 100 – 2000  $\mu\text{m}$ , normally referred to as microspheres. These microspheres can then be poured directly into the fuel pin, and this is commonly referred to as a sphere-pac type of fuel [BAR 08]. It is also possible to produce fuel elements where the microspheres are dispersed in a graphite matrix [CHA 08]. Traditional pellet-based nuclear fuel can also be produced from microspheres by conventional pellet pressing. These spheres are produced by a set of wet chemical techniques known as sol gel. The basis for sol gel chemistry within the nuclear fuel field is the solidification of actinide solutions by forced gelation/precipitation in the form of small spheres or droplets. The spherical shape is obtained by presenting the start sol to an immiscible medium such as organic diluents or gas phase. The different sol gel production techniques for nuclear fuel microspheres are external gelation, internal gelation, IChTJ and the double extraction process. One of the main advantages of using sol gel techniques for nuclear fuel fabrication is that the microspheres produced pose a smaller radiotoxic hazard than when working with powder materials [GAN 93].

## 2.5. Introduction to sol gel techniques for nuclear fuel production

In the external gelation process the sol consists of an actinide solution and possibly viscosity and surface tension-modifying agents such as polyvinylalcohol (PVA) and tetrahydrofurfuryl alcohol [FU 04, VER 07]. The sol is pumped through a nozzle to break it up into droplets. The droplets subsequently fall through an ammonia-containing gas phase. The ammonia reacts with the surface of the droplet resulting in a rapid pH increase in the droplet surface. This pH increase causes the metal ions in the droplet to hydrolyze and form a protecting shell on the droplet surface. The surface gelled droplets then fall into an  $\text{NH}_4\text{OH}$  (aq) solution where diffusion of  $\text{OH}^-$  into the microspheres causes all metal ions inside to solidify.

The IChTJ process starts from a metal nitrate and citric acid solution. The start sol is pH-calibrated to around 4. The sol is then emulsified in dewatered 2-ethyl-1-hexanol (2EH) containing a nonionic surfactant called SPAN 80. Water is extracted into the 2EH, forcing the metal ions in the sol emulsion droplets to gel once the water content in the droplets has become too low to support a solution [BRY 14].

The double extraction process works very similarly to the IChTJ process and is basically an extension of it [BRY 14]. The difference is that in the double extraction process a rather long-chained primary amine is mixed into the 2EH. The amine coextracts nitrates during gelation. The idea in extracting nitrates from the sol during gelation is to reduce the tendency for the produced microspheres to fracture during subsequent heat treatments. Nitrate constitutes a problem during heat treatment since it can rapidly decompose into gaseous products. The gas products can then cause mechanical damage on the microspheres as they escape out into the surrounding atmosphere.

In the internal sol gel technique the start sol is a metal nitrate solution to which gelation chemicals are added. The gelation chemicals added are urea and hexamethylenetetramine (HMTA). Just as in the external gelation process the sol is then dripped through a nozzle. The difference is that in the internal gelation process the sol is dripped into an organic diluent, typically silicone oil. The silicone oil is heated up to typically between 50 and 100 °C, depending on sol composition [VAI 08, POU 09], and the heat causes HMTA to chemically decompose. The HMTA decomposition raises the pH in the solution and induces a gelation reaction. It is the internal sol gel process that has been studied within the scope of work in this thesis.

## 3. Theory

### 3.1. Nitrides as a nuclear fuel ceramic

Nitrides have long been considered to be a candidate material for use as nuclear fuel. The reason for this is that nitrides possess several properties that are beneficial for a nuclear fuel to have, such as high thermal conductivity, high melt temperature, high fissile material density and compatibility with liquid metal coolants such as sodium and lead.

A nuclear fuel does not necessarily have to be completely composed of actinide-containing chemical compounds such as UN or PuN. In order to lower the amount of, for example, Pu in a ceramic nuclear fuel material such as PuN, a second inert phase can be added. Such a fuel is then defined as either a CERCER (ceramic in ceramic) fuel, which is a fuel type where the solid fuel diluent is another ceramic, or, if the solid diluent is a metal, the fuel is called a CERMET (ceramic in metallic) fuel. The combined name for these types of fuel is inert matrix fuels (IMFs).

ZrN is one material suggested as a solid diluent material for nitride-based nuclear fuel [KLE 99]. Just as UN and PuN, ZrN crystallizes within the FCC–NaCl structure and the UN, PuN and ZrN system possess the benefit of forming solid solution materials instead of a phase-separated matrix [GAN 97, STR 03, KLE 99, HOL 68]. ZrN also displays high thermal conductivity, allowing it to be utilized as an inert matrix without compromising the heat transfer benefits that actinide nitride fuels offer. ZrN has also been shown to be compatible with liquid sodium, which is one of the candidate coolants in LMFBRs. Mixed (Zr,Pu)N fuel is of interest for reactor design due to its favorable neutron economy during in-core operation [WAL 09].

#### 3.1.1. Thermal conductivity of nitrides

As can be seen in Table 1, uranium and plutonium nitrides have much higher thermal conductivity than the corresponding oxides, typically around a factor 10 higher. High thermal conductivity is a property which is shared also by zirconium nitride. The nitride form of U, Pu and Zr, also displays an increase in thermal conductivity with increasing temperature [ARA 98, CIR 09]. The difference in thermal conductivity between the oxide and nitride form during reactor operation will be that the temperature gradient within a nitride based nuclear fuel will be much smaller than in the oxide case. A lower temperature gradient within the fuel pellets consequently results in a lower center temperature of the fuel pellets. Together with the fact that the nitrides have melting points that are equal to or surpass those of the oxide forms [KLE 99, HAY 12], this means that there will be a larger temperature safety gap between the centerline operation temperature and the melting temperature of the fuel.

#### 3.1.2. Melting temperature

The melting temperature of UN, PuN and ZrN is not fixed but both temperature and the melting process itself depend on the partial pressure of N<sub>2</sub> in the surrounding atmosphere

[KLE 99, OLS 63, OET 67, OLS 64]. At one bar of N<sub>2</sub> neither UN nor PuN melts but they decompose, the decomposition temperature being 2780 °C for UN and 2570 °C for PuN. At a pressure of three bar UN has a congruent melting point of 2830 °C while PuN melts incongruently at three bar N<sub>2</sub>. ZrN is reported to melt at 2960 °C.

### 3.1.3. Drawbacks of nitrides

Several drawbacks of nitride-based nuclear fuels have also been pointed out and are worth mentioning. First of all there is the problem of <sup>14</sup>C production in nitride fuels during reactor operation. The <sup>14</sup>C produced in the reactor can be taken care of during reprocessing and solidified and bound as carbonates and diluted out in, for example, concrete. This, however, produces a new waste fraction that must be managed. Fourth-generation reactor systems and fuel cycles aim at lowering the radio-toxicity and required storage time of the finally produced waste. It would thus somehow go against its own purpose to use a fuel that gives rise to an additional radioactive waste fraction. The <sup>14</sup>C problem arises from the fact that <sup>14</sup>N produces <sup>14</sup>C by (n,p) reaction. The consumption of neutrons when using <sup>14</sup>N also lowers the neutron economy of the system compared to when using oxide-based ceramic fuels [MAT 91]. These problems can, however, be overcome by producing nitrides using <sup>15</sup>N enriched nitrogen, and thereby counteracting the production of <sup>14</sup>C and improving neutron economy. The downside is that the <sup>15</sup>N constitutes only a small fraction of the nitrogen in the atmosphere and the cost of producing and recovering the enriched <sup>15</sup>N is added to the fuel production cost.

The production of nitride-based nuclear fuel is also somewhat inconvenient. The nitrides are not stable towards oxidation by air, so that manufacturing has to be performed under inert atmosphere conditions. There is also a problem regarding pyrophoricity when working with nitride powders. This is a problem that can be diminished by avoiding working with fine powders. One way to minimize powder handling would be to avoid having powders at all during process handling. This can be accomplished, for example, by producing microspheres as fuel pellet precursors by sol gel techniques.

In water-cooled reactors nitrides could in theory be utilized as chemical form of the fuel but actinide nitrides such as pure UN are not stable towards water at elevated temperature. Degradation of UN into UO<sub>2</sub> and NH<sub>3</sub> would destroy the fuel in the event of a rupture of a cladding tube [RAM 91].

When producing nitride-based nuclear fuels it is also important to minimize remaining contaminants in the nitride such as carbide and oxide. The dissolution properties of nitrides have not yet been thoroughly studied, but oxides contribute to making the dissolution of the fuel more difficult during reprocessing. Carbon can be a problematic element during in-pile operation. During swelling if the fuel comes into contact with the cladding, carbon can migrate to the cladding material. This carburization process of the cladding material causes embrittlement and reduced mechanical strength of the cladding tube.

### 3.1.4. Nitride production techniques

There are several different ways of producing nitrides such as hydriding/nitriding reactions. This is a technique that utilizes metals as starting material. Reactive ball milling is a technique which also uses metals as starting material. Oxidative ammonolysis is a method that starts from metal oxides. Carbothermal reduction is a process that also uses metal oxides as starting material and is considered to be the only economically feasible reaction route for large-scale processing [BER 89].

During the hydriding/nitriding process the metal used is first heated in a hydrogen-containing atmosphere, typically  $H_2$  in Ar. The formed hydride has a lower density than the metal, which causes the volume of the material to increase and hydride to fall off the metal as powder, exposing new metallic surface to the reaction gas. The hydride is then converted into nitride by either direct reaction of the hydride with nitrogen gas at elevated temperatures or by dehydriding to metallic state in an inert atmosphere followed by nitridation of the metallic powder in  $N_2$  gas [OI 72]. When ZrN is produced by this method a milling step is required since hydriding of zirconium metal forms  $ZrH_2$  which is a very brittle material but does not automatically form a powder, unlike when hydriding for example uranium [PAR 11].

Reactive ball milling is a technique where the metal is milled into a fine powder under a nitrogen atmosphere. Formation of nitride using this method has been shown to work when milling at room temperature and atmospheric pressure of  $N_2$ , however the ball to material ratio used is however quite high and long milling times are required [SHE 00].

Oxidative ammonolysis is a production route that starts from metal oxides rather than metals. It has been proven to work for the synthesis of UN from  $UO_2$  [YEA 08]. The process is carried out by mixing  $UO_2$  with  $NH_4HF_2$  to produce  $(NH_4)_4UF_8$  at room temperature. The  $(NH_4)_4UF_8$  is then reacted with  $NH_3$  at elevated temperature to produce  $UN_2$  and denitrated to UN by heating in an argon atmosphere.

The carbothermal reduction process starts from metal oxides and elemental carbon. Nitrides are produced by heating this mixture in an  $N_2$  or  $N_2 + H_2$  atmosphere. The metal oxide and carbon can be directly mixed as powders and pressed into thin clinkers prior to carbothermal reduction. This does, however, require the metal oxide to be handled in powder form. Powder handling would then be required both during mixing with carbon and when pressing fuel pellets. This is because the produced thin nitride discs would have to be ground before pelletization. One method to avoid this powder handling is to produce microspheres by a sol gel process. Through this process it is possible to produce microspheres that contain both the carbon material and the metal oxide at the same time. Microsphere production through sol gel processes also minimizes the requirement of powder handling.

### 3.2. Internal Sol Gel

The internal sol gel process was originally developed in the KEMA laboratories in the Netherlands [KAN 74, BRU 70]. The process was developed for production of UO<sub>2</sub> fuel kernels. In the internal sol gel procedure, the gelation agents are added to the sol gel feed broth. By contacting the sol with an immiscible heat transfer agent such as silicone oil the gelation chemicals are thermally degraded. This thermal degradation causes an increase in pH to occur and the pH increase starts the gelation of the metal nitrate solution. The fact that the gelation chemicals used in the internal sol gel process are degraded by heat requires the sol to be prepared at low temperature, typically 0 – 4 °C [VAI 87]. The sol is dripped from a nozzle either down into a stationary bath of heated silicone oil or into a heated laminar flowing oil stream. The nozzle is used to form droplets which upon gelation form solid spheres, commonly referred to as microspheres.

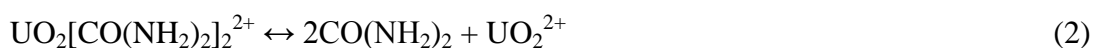
The gelation chemicals used in the internal sol gel process are urea and hexamethylenetetramine (HMTA). The urea is added with the purpose of forming stabilizing complexes with the metal ions, preventing premature gelation. When the sol is heated in the silicone oil the urea decomposes and HMTA degrades and thus induces gelation of the sol [APA 12]. In order to minimize the gelation chemicals needed in the gelation step, acid deficient uranyl nitrate solution (ADUN) is often used as starting metal nitrate solution [VAI 87]. A stoichiometric uranyl nitrate solution has a nitrate to uranium molar ratio of two. In ADUN the nitrate to uranium ratio can be varied between about 1.5 and 2.

There are several different parameters that are of importance when preparing microspheres according to the internal sol gel procedure. Among the more obvious ones are of course the concentrations of metal nitrate, urea, and HMTA as well as carbon source material. Several different types of carbon additives have been utilized as carbon source and include graphite powder (roughly 10 µm size particles, Acros Organics), carbon nano powder (CNP) (particle size around 200 nm, Supelco), multi-walled carbon nanotubes (CNT) (size 5 µm in length and 6 – 9 nm in outer diameter, Aldrich) and sucrose as a carbon source dissolvable in the sol.

Other parameters that are of importance to the microsphere preparation are what temperature is used for the oil heating bath, what kind of and what amount of concentration of dispersing agents is used (if any) for obtaining a good suspension of the carbon material, what kind of oil is used as heat carrier, if any vibration of the nozzle is being used and at what frequency.

Uranium is the element that has been most thoroughly studied in the internal sol gel process, and the main reaction steps when the sol is heated are [COL 87]

Decomplexation of urea



Hydrolysis of the uranyl ions



HMTA protonation



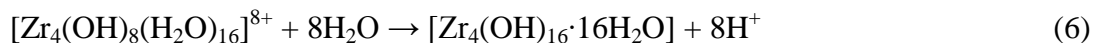
HMTA decomposition



where consumption of  $\text{H}^+$  by HMTA is the mechanism which drives the reaction forward.

The formation of the monomer  $\text{UO}_2\text{OH}^+$ , dimer  $(\text{UO}_2)_2(\text{OH})_2^{2+}$  and trimer  $(\text{UO}_2)_3(\text{OH})_5^+$  species of the hydrolyzed uranyl ion have also been reported to form during the hydrolysis reaction, indicating that this is at least partially a polymerization reaction and not just a precipitation. These oligomers are also present in the ADUN solution when the gelation chemicals have not been added; when HMTA is used as hydrolysis agent the dominantly formed oligomer is the trimer. The formed microspheres also contain the protonated HMTA molecule  $[(\text{CH}_2)_6\text{N}_4\text{H}]^+$  incorporated as intercalated cations in the gel [KIN 90]. Washing of the produced microspheres is necessary before drying. First the microspheres are washed typically in  $\text{CCl}_4$  or petroleum ether to remove silicone oil from the surface of the microspheres. A second washing in  $\text{NH}_4\text{OH}$  (aq) is then performed in order to remove unreacted HMTA, urea and  $\text{NH}_4\text{NO}_3$  from the microspheres. If the residual gelation chemicals are not washed out from the microspheres there is an increased problem with cracking of the microsphere during drying and subsequently also during heat treatments when the residual chemicals are gasified if not removed [HUN 10]. Ageing of the produced microspheres in  $\text{NH}_4\text{OH}$  is also performed in order to make sure that all metal in the microspheres is gelled / precipitated. During washing and ageing of the microspheres in  $\text{NH}_4\text{OH}$  the  $[(\text{CH}_2)_6\text{N}_4\text{H}]^+$  ions are exchanged for ammonium ions and the structures present in the microspheres become  $\text{UO}_3 \cdot 2\text{H}_2\text{O}$ ,  $\text{UO}_3 \cdot 0.25\text{NH}_3 \cdot 1.75\text{H}_2\text{O}$  and  $2\text{UO}_3 \cdot \text{NH}_3 \cdot 3\text{H}_2\text{O}$  [KIN 90, LLO 76].

The gelation procedure of zirconium-containing sols in the internal sol gel process has not been as extensively studied as the gelation reactions for uranium containing sols, but it has been suggested that zirconium is solidified in the form of hydrated zirconium hydroxide from zirconium tetramers in the sol [BEN 08, HAG 04, TSU 99]



When producing americium-bearing microspheres the ageing step in  $\text{NH}_4\text{OH}$  is of importance in order to induce the americium to precipitate in the gel. The americium does not coprecipitate together with the uranium and plutonium, but during washing and ageing the americium will precipitate in the pores of the gel structure. The coprecipitation behavior in zirconia gels is yet to be investigated [LED 96].

No detailed chemistry for the gelation of microspheres from only plutonium containing sols has been encountered in the literature regarding the internal gelation process. Work has been performed at ORNL on pure plutonium sols, but it has done been on the extraction principle where water and  $\text{HNO}_3$  is removed from the droplets, thereby forcing a gelation to occur [LLO 78].

The internal sol gel process can be used as the primary step for producing different kinds of nuclear fuel ceramics such as oxides, nitrides or carbides when starting from a metal nitrate solution. When making oxide microspheres with the internal sol gel process, it is sufficient to prepare a sol containing metal nitrate solution plus gelation chemicals. Carbon particles can be optionally added to the sol to act as a pore-forming agent during subsequent calcination during oxide microsphere production. When the aim is to produce nitrides or carbides from the microspheres obtained by the internal sol gel procedure, a carbon source is required to be added to the sol in order to be able to convert the produced oxide microspheres into nitrides/carbides by carbothermal reduction. If carbide production is intended the carbothermal reduction is performed under an inert atmosphere or vacuum. Nitride production is performed under a non-oxidizing,  $\text{N}_2$  containing atmosphere [TAN 94]. In order to get the carbon dispersions to be more stable during the gelation process, additives that work as dispersion agents can be used in order to increase the stability of the particle suspension.

### **3.3. Dispersion agents and carbon dispersion**

A dispersion agent is a substance that facilitates and/or improves the separation of solid particles in a solution. Typically either surfactants or block copolymers, or a combination of these, are used as dispersants. There are two main mechanisms for increasing dispersion stability, steric and electrostatic repulsion. Both repulsion mechanisms work by counteracting a decrease in entropy that arises when the ions or the ethylene oxide chains on the particle surfaces approach each other [HOL 03].

There is a need to increase the dispersion efficiency of the particle based carbon material introduced into the sol (i.e. not sucrose but all solid non-dissolvable carbon species). Carbon nanotubes are, for example, by nature very poorly dispersed in aqueous solutions without any chemical additions. If the carbon material utilized in the sol is not efficiently dispersed, settling of the material will occur in the gelation process. The produced microspheres will then have a very uneven carbon distribution, which will affect the nitridation by carbothermal reduction of the microspheres.

### **3.4. Carbothermal reduction**

In analogy to the case with the internal sol gel process, the carbothermal reduction step for making UN and mixed (U,Pu)N from carbon containing oxide microspheres is studied more closely and in higher detail than the corresponding reactions for producing ZrN and (Zr,Pu)N.

When producing uranium nitrides by the internal gelation process, microspheres formed in the gelation step will be approximately in the form of  $\text{UO}_2(\text{OH})_2$ . The microspheres have to be converted into oxides before carbothermic reduction and formation of uranium nitride can be performed. The hydroxides can be converted into oxides by heating in an inert atmosphere. However, for materials where higher oxidation states can exist than the dioxide, such as uranium oxides, there is a need to adjust the oxidation state and form the dioxide before carbothermal reduction is possible. Reduction to stoichiometric dioxide can be performed by heat treatment in a hydrogen-containing reducing atmosphere according to reaction 7 [LED 92].



The drawback of using hydrogen to reduce higher uranium oxides to  $\text{UO}_2$  is that a certain loss of carbon from the microspheres can occur due to reaction 8 [MUK 93].



An alternative possibility to produce stoichiometric  $\text{UO}_2$  is to use an over-stoichiometric amount of carbon in the microspheres and form  $\text{UO}_2$  by the overall reaction [MUK 90, MUK 91].



Carbothermal reduction is then subsequently performed on the carbon containing metal oxide microspheres. The reaction can be performed in a variety of atmospheres like pure  $\text{N}_2$ ,  $\text{N}_2\text{-H}_2$  mixtures and  $\text{NH}_3$  [MUK 91, GAN 91, ALL 67, MUR 77].

When carbothermal reduction is performed on  $\text{UO}_2$  in pure  $\text{N}_2$  at atmospheric pressure and temperatures below around 1723 K, the overall nitride formation proceeds according to reaction 10 [MUK 91].



If the temperature is higher than 1723 K a carbonitride intermediate material will form according to reaction 11 [MUK 91].



If heating is continued after the carbonitride is formed, elimination of carbon from the structure continues through reaction 12.



Reaction 12 is, however, only driven forward if the formed carbon is removed either by reaction with residual  $\text{UO}_2$  or by reaction with hydrogen.

From the carbonitride state, carbon can be removed by reaction with hydrogen and formation of short-chain hydrocarbons, illustrated in reaction 13 as methane.



Free elemental carbon can also be removed by formation of hydrogen cyanide if hydrogen is present in the reaction gas [BAR 92]

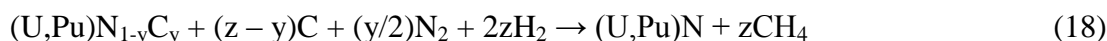


The HCN can in turn react further, forming cyanogen and cyanamide



Elemental carbon may be reformed according to reaction 16. However, it is clear that the unwanted formation of elemental carbon can be minimized by removal of hydrogen cyanide and cyanogen in the reaction gas flow.

Carbothermal nitridation studies have also been performed on mixed  $\text{UO}_2$ ,  $\text{PuO}_2$  materials, and the reaction mechanisms that have been suggested show great similarities to those of nitridations of pure  $\text{UO}_2$  [PAU 88], see reactions 17 and 18.



The nitridation reaction can also proceed by direct reaction between metal oxide and hydrogen cyanide [BAR 92]



The carbothermal reduction process for producing nitrides from zirconium oxides has been studied by Pialoux et al. [PIA 91] and several different temperature-dependent reactions have been proposed.

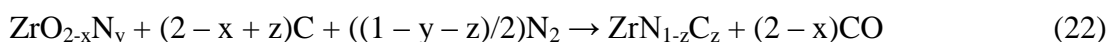
The first part of the reaction is the formation of oxynitride in the temperature range  $1423 \leq T \leq 1883$  K by the reaction



The reaction can then proceed by direct nitride formation in the temperature range  $1673 \leq T \leq 1783$  K if graphite carbon is used as carbon source by



If the temperature exceeds 1783 K there will instead be formation of carbonitride by



## **3.5. Pelletization and Sintering**

### **3.5.1. Pelletization**

Pellet pressing is performed by mechanical compaction of a starting material that consists of freely moving entities such as powders, granulates or microspheres. The material to be pelletized is put into a pressing die and a plunger is inserted into the die and pressed onto the sample. The mechanical compaction causes the individual particles in the free-flowing material to be forced close enough to each other that an adhesive force arises between the different particles. In the case of pressing pellets from microspheres or some sort of granulate, for example, the compaction pressure causes more or less destruction of the initial material to reach any higher levels of adhesive strength between the particles in the formed pellet. The newly pressed, often mechanically quite weak body is normally referred to as a green pellet.

If there are difficulties in forming a green pellet of desired density and mechanical strength, additives can be used to improve the performance during pressing. The additives may serve different purposes such as acting as a binder between the particles to increase strength or acting as a lubricant for facilitating pressing without equipment becoming stuck in the pressing die. Additives can also be added in order to improve sintering characteristics.

### **3.5.2. Sintering**

Sintering is a process that is based on heat-induced densification of solid materials. The thermodynamic driving force for sintering phenomena is minimization of surface free energy by consolidation of grain boundaries. Three driving mechanisms for sintering are [RAH 03]:

- Curvature of the particle surfaces
- Externally applied pressure
- Chemical reactions

These mechanisms are the reason that causes sintering to occur, but the physical densification itself is facilitated by movements of atoms within the material structure. In crystalline solids there are always defects present in the otherwise ordered structures, and it is through the defects that atomic transport mainly takes place. The equilibrium defect density in a crystalline material is dependent on the temperature of the material. Since the lowest possible energetic state in a crystal structure is a perfectly ordered one, the thermodynamic driving force for forming defects in a crystal is lowering of free energy by increase in entropy [SMA 05].

Crystalline materials normally contain different types of defects, which can be categorized as [RAH 03]:

- Point defects

- Line defects
- Planar defects

When spherical particles adjacent to each other sinter together, they do so by neck growth. In practice, this means that the particles sinter together at their respective contact points to one another, forming “necks”. There are several different kinds of mass transport mechanisms during this kind of neck growth but only some of them lead to densification of the material.

The mass transport mechanisms are [RAH 03, RIE 11]:

- Surface diffusion
- Lattice diffusion from particle surface to the neck
- Vapor transport
- Grain boundary diffusion
- Lattice diffusion from the grain boundary
- Plastic flow

Out of these mechanisms, the first three are non-densifying mechanisms. This means that they do lead to neck growth between grains but they do not transport material to pores forming between the neck growth areas of particle clusters. The grain boundary diffusion and lattice diffusion from the grain boundaries are mechanisms that do promote translation of material from the grain and neck boundary towards the pore. The plastic flow mechanism also leads to neck growth and densification during sintering but is more commonly observed during metallic sintering than ceramic [RAH 03]. Figure 2 illustrates schematically the 6 different material transport mechanisms possible when sintering spherical objects.

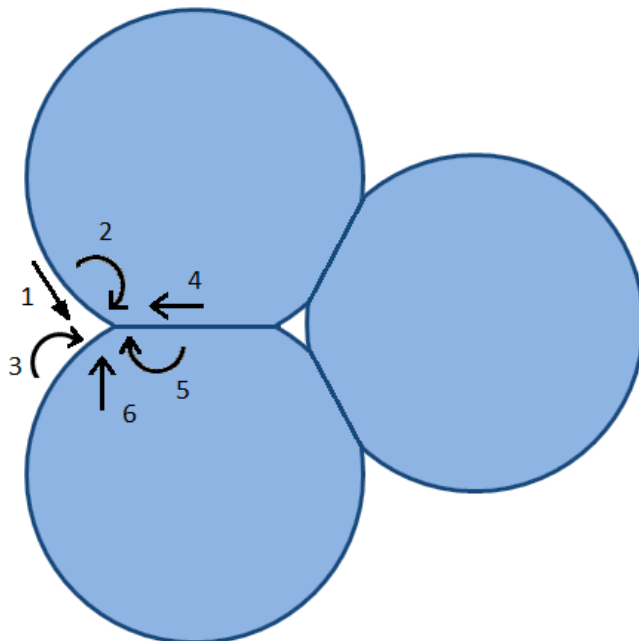


**Figure 2.** Schematic picture indicating the transport mechanisms occurring during sintering. The different arrows indicate 1 Surface diffusion, 2 Lattice diffusion from the surface, 3 Vapor transport, 4 Grain boundary diffusion, 5 Lattice diffusion from the grain boundary and 6 Plastic flow [RAH 03].

## **3.6. Characterization**

### **3.6.1. Scanning Electron Microscopy and Energy dispersive X-ray Spectroscopy**

Scanning Electron Microscopy (SEM) is a technique for imaging of surfaces with the use of an electron beam. The electron beam is normally generated by heating a tungsten filament. The emitted electrons are then accelerated by an electric field to a kinetic energy of about 10 – 20 keV. The sample that is to be investigated is normally attached to a sample holder using an adhesive carbon tape. The sample is subsequently inserted into a measurement chamber and the chamber is evacuated. The advantage of using an electron microscope compared to a traditional optical microscope is that the very small wavelength of an electron material wave can provide a higher resolution compared to an optical microscope. In a scanning electron microscope the image is generated by moving a focused electron beam back and forth over the sample. The electrons leaving the sample surface contain information about the surface that with mathematical treatment can be converted into an image of the surface. There are two different possible electron imaging techniques when running SEM, back-scattered electron imaging and secondary electron imaging. When using secondary electron imaging techniques, the electrons detected and used for producing the image originate from the measured sample and are ejected from the sample by energy transfer from the scanning electron beam. The back scattered electron detection technique produces the image by detection of the electrons that ricochet back from the surface. The back scattering probability of an incoming electron increases with the atomic number of the atoms on the analyzed surface. Therefore this detection technique can produce a contrast difference in the image if the analyzed sample is made up of separate regions of different atomic species. The result will be that an area consisting of heavier atoms such as uranium will produce a brighter image compared to an area containing, for example, zirconium.

Energy dispersive X-ray spectroscopy (EDX) analyzes and quantifies the elemental composition of the scanned surface by identifying characteristic X-rays emitted from the atoms on the surface. The X-rays are generated during de-excitation of valence electrons to low energy states in the atoms. The low-energy states become unoccupied when enough energy from the electron beam is transferred to inner orbital electrons to allow them to overcome the energy potential barrier that binds them to the atom nucleus. The emitted X-rays will thus be of specific energies unique to every element in the periodic table. When electrons accelerate they emit light. The deceleration of electrons upon impact with the investigated material surface will therefore give rise to additional X-ray emission. These X-rays are commonly referred to as bremsstrahlung. The bremsstrahlung overlaps with the low energy X-ray region of the EDX spectrum resulting in increased difficulty for accurate identification and quantification of measured X-ray peaks in the low-energy region of the EDX spectrum.

### 3.6.2. SEM/EDX measurements

The scanning electron microscope used for SEM characterization was a Hitachi TM 3000 with a back scatter electron detection system. This electron microscope scans in the X, Y plane, but the electron beam is stationary in Z direction. The sample holder was therefore height-adjusted in accordance with the microscope specifications before insertion into the microscope in order to obtain good focus of the electron beam. The microspheres were mounted on the aluminum sample holder using a carbon adhesive tape. When doing microscopy on pressed pellets no tape was used. The pellet was put directly on the aluminum sample holder.

The EDX measurements are performed during SEM characterization. The sample preparation was thus the same as for the SEM sample preparation. The software used for EDX measurements and data handling was Quantax 70. For calibration of the EDX energy spectrum copper metal tape was used as reference material.

### 3.6.3. X-ray diffraction

X-ray diffraction (XRD) is a technique where the crystal structure of a material can be determined using X-rays. When monochromatic X-rays hit the sample surface a constructive diffraction pattern can arise in the reflected X-ray beam depending on the angle of the incoming X-ray beam. What angles give rise to constructive interference is determined by the wavelength of the X-rays and the spacing between the diffracting planes in the crystal as dictated by Bragg's law. Depending on the crystal structure and the atomic distances in the measured material, constructive interference will arise at different angles producing an angle-dependent diffraction spectrum. Traditionally the measurement angle  $\Theta$  is plotted as  $2\Theta$  in the diffractogram. This spectrum can be thought of as a sort of a "thumb print" for the material investigated. If several different crystalline species are present in the sample measured, separate diffraction peaks will arise for every crystal structure present. The crystalline compounds present in concentrations higher than about 2 weight% in a mixture can be identified by comparison with standard data in the Joint Centre for Powder Diffraction Standards database [JCP 13].

Materials with the same crystal structure and similar inter-atomic distances can be difficult to identify separately by XRD. In addition, they can be present as solid solution instead of phase-separated crystal structures. An example of such a material combination would be ZrN and ZrC, which both crystallize within the FCC-NaCl type of structure. In a substitution solid solution the N and C atoms would be randomly distributed over the octahedral sites occupied by both atom species in the FCC-NaCl structure. In this case the diffraction pattern would not show the diffraction peaks of each separate chemical compound since both the nitride and carbide coexist in the same crystal structure. Instead one set of diffraction peaks would be obtained, but the peak angles would be shifted to positions between those of the diffraction peaks of the respective carbide and nitride. The chemical composition of the solid solution would influence how large the peak shift would be from the pure substances. For example, a

solid solution with the composition  $Zr(N_{0.9}C_{0.1})$  would produce peaks rather close in angle to that of pure ZrN while  $Zr(N_{0.1}C_{0.9})$  would be shifted much closer to the peaks of pure ZrC.

In cubic crystal systems all side lengths of the smallest repeating unit defining the crystal structure will be the same. For a cubic crystal system it is thus possible to define a lattice parameter which defines the side length of the repeating cube. Two different chemical compounds crystallizing within the same cubic crystal structure such as ZrC and ZrN will thus still have different lattice parameters. Lattice parameters are estimated by calculation from individual peaks at high angles and averaged from the results. The peaks utilized for lattice parameter determination should occur at sufficiently high  $2\Theta$  angle to be able to distinguish between the  $k_a$  1 and 2 peaks for maximal precision. Since the diffraction peaks shift with changing composition of a solid solution, the lattice parameter can thus be used to estimate the chemical composition of the measured material. It should be kept in mind, however, that XRD is a surface-sensitive technique. Therefore the chemical composition obtained by this type of methodology provides an estimate of the surface composition, which may differ from the actual composition of the material in the bulk.

One way to estimate the composition of a solid solution by determination of lattice parameter is to perform a linear interpolation between the lattice parameter of the compounds in the solid solution. This is known as Vegard's law. For a binary solid solution compound Vegard's law is mathematically expressed as

$$a = a_A^0(1 - X) + a_B^0X \quad (\text{eq. 1})$$

where  $a$  denotes the lattice constant of the sample,  $a_A^0$  the lattice constant of pure substance A,  $a_B^0$  the lattice constant of pure substance B and  $X$  the molar fraction of substance B in the sample.

The problem with Vegard's law is that even if an idealized solid solution is to be considered, Vegard's law cannot be considered a true relation but can only be regarded as an approximation [JAC 07]. Bearing this in mind, Vegard's law can still be used for estimations of chemical composition, especially in cases where the considered material consists of a dominant part of one of the compounds in the solid solution and the second compound is present in lower mole fractions.

#### **3.6.4. XRD measurements**

XRD measurements have been performed on produced nitride pellets. The instrument used was a BRUKER D2 PHASER. The measured sample was placed in a sample holder. No height-adjusting mechanisms were available either on the sample holder or in the XRD measurement chamber. Therefore no exact equalization of the sample and holder height was possible. An inlay in the sample holder was used to correct the pellet surface heights, but since the produced pellets are of only approximately the same size the height correction was not optimal for every pellet measured. The height difference between the sample holder edge and the sample surface varied within  $\pm 1$  mm.

Monochromatic Cu  $k_{\alpha}$  X-rays were used in measuring the sample. The rotation speed of the sample holder was  $360^{\circ}/\text{min}$ . For identification of characteristic peaks a measurement angle interval of  $20 - 80^{\circ} 2\theta$  was used. When obtaining data for determination of lattice parameters, the measurement angle interval was increased to  $20 - 150^{\circ} 2\theta$ .

### **3.6.5. Analytical methods for light element quantification**

Quantification of elemental composition regarding light elements such as H, N, O and C can be performed by combustion techniques. The measurements that have been performed using these techniques have utilized analytical equipment produced by LECO Corporation. The methods described within this section therefore focus on the principles that the used equipment utilizes. The descriptions and detection methods mentioned are thus not necessarily universal for every kind of combustion.

Determination of carbon content in a sample can be performed by combustion of the sample with oxygen as carrier gas. The carbon forms CO and CO<sub>2</sub> and before detection using catalyzer to form CO<sub>2</sub> which is then detected by infrared absorption.

Determination of N, O and H is performed by degassing the elements at high temperature in an inert gas stream such as argon or helium. When measuring, the sample is placed in an aluminum foil. The foil is subsequently put in a nickel coil. The nickel coil will aid the sample to melt properly during heating in an inert atmosphere. The foil + coil sample is put in a graphite crucible which is inserted into the measurement apparatus. During heating the nitrogen in the sample will form N<sub>2</sub> while H and O will form chemical species such as H<sub>2</sub>O, CO and CO<sub>2</sub>. The oxygen and hydrogen containing species are detected by infrared absorption while N<sub>2</sub> is detected by heat conductivity measurements of the flowing gas stream.

## 4. Experimental procedures

### 4.1. Preparation of zirconium sols

When producing sols for gelation of zirconium containing microspheres, zirconylchloride tetrahydrate ( $\text{ZrOCl}_2 \cdot 4\text{H}_2\text{O}$ , Alfa Products) was dissolved into MQ water (18.2 M $\Omega$ ). Then carbon containing material was added to the solution. To get the  $\text{NO}_3^-/\text{Zr}$  ratio to the desired level  $\text{HNO}_3$  (Sigma – Aldrich) was added to the solution. To increase the stability of the particle dispersions a dispersion agent was added to the solution, the dispersion agent that has been most commonly used during experiments is Triton X-100 (t – octylphenoxypolyethoxyethanol, Sigma-Aldrich), which is a non-ionic surfactant. Normally ionic surfactants are considered to be more efficient dispersion agents than non-ionic ones, and there are ionic surfactants that can disperse higher amounts of CNT than Triton X-100, can such as sodium dodecylbenzene sulfonate [ISL 03]. The reason for choosing a non-ionic surfactant instead of an ionic one is that the ionic surfactants becomes ineffective in solutions containing high salt concentrations due to screening effects of the electrical double layers forming when the surfactants adsorb onto the particle surfaces.

The sol is cooled to 4 °C and mixed by magnetic stirring before addition of urea (Sigma – Aldrich) and HMTA (Aldrich) was started. Urea is added first and allowed to dissolve completely before HMTA is added; a urea/Zr ratio of 2 has been used in the gelation experiments where zirconium gels have been produced. The HMTA/Zr ratio used during gelation experiments was 0.7, and the HMTA was added by small amounts at a time to allow it to be mixed into the sol. The HMTA dissolved rather slowly in cold aqueous media, and rapid addition of HMTA resulted in a large lump of HMTA instead of fine particles and dissolution times became considerably longer than expected.

The experimental set-up of the internal sol gel equipment used during gelation experiments is presented in Figure 3.

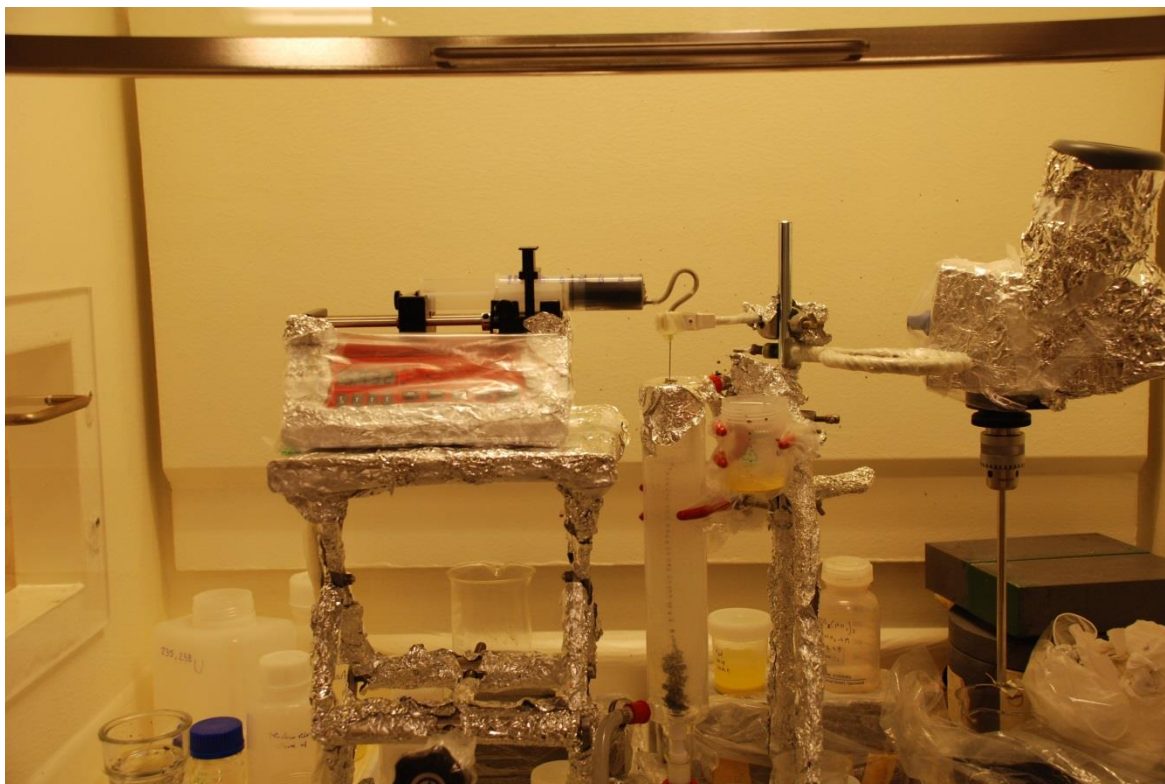


**Figure 3.** The experimental set-up of the inactive/low-active internal sol gel equipment.

Experiments have been carried out by mounting a syringe filled with the cooled sol gel feed broth into the syringe pump and pumping the sol through a nozzle, forming droplets that fell down into the heated silicone oil container. The pump speed investigated during gelation experiments was varied between 10 and 25 ml/h.

During some experiments a permanent magnet vibrator was connected to the nozzle in order to produce smaller droplets and control the size of the formed microspheres. The frequency of the oscillations was varied between 0 and 100 Hz.

## **4.2. Water migration to the silicone oil**

An experiment was performed in order to establish if the addition of surfactant to the sol caused migration of water residing in surfactant micelles into the oil. A sol consisting of water CNT and Triton X-100 was contacted with Rhodorsil silicone oil 1000 (cSt) heated to 90 °C and mixed for a few minutes. The produced slurry was left to cool and phase separate. Samples of the silicone oil were withdrawn and density was measured using a calibrated density probe (SIGMA, 701) and a microbalance. The density measured was then compared to that of unused silicone oil whose density had been measured using the same equipment.

### **4.3. Preparation of uranium containing sols**

Several different methods to prepare ADUN solution was investigated; dissolution of  $\text{UO}_2$  in  $\text{HNO}_3$ , dissolution of  $\text{U}_3\text{O}_8$  in  $\text{HNO}_3$  and dissolution of uranyl nitrate ( $\text{UO}_2(\text{NO}_3)_2 \cdot 6\text{H}_2\text{O}$ , Fluka Analytical) in MQ followed by  $\text{NO}_3^-/\text{U}$  ratio correction by addition of  $\text{UO}_3$  (produced in-house) to the solution.

Several different gelation conditions with respect to urea and HMTA addition were investigated. The work of Vaidya et.al. [VAI 87, VAI 08] was used as a reference for gelation field diagrams regarding the U, urea and HMTA composition of the sols. No carbon addition, and thus no surfactant, was used when making sol gel on the uranium based sols; otherwise the preparation of the sol followed the same general procedure as during preparation of the zirconium sols. The sol was cooled down to  $4^\circ\text{C}$  before urea and HMTA was added, and identical silicone oil was used in the gelation column.

### **4.4. Nitridation of zirconium microspheres**

When nitriding the formed zirconium containing microspheres, the dried microspheres were placed in a molybdenum metal crucible and placed in a graphite resistor-heated high-temperature furnace with a maximum operating temperature of  $2500^\circ\text{C}$  (Figure 4). The furnace temperature regulation consisted of a molybdenum thermocouple up to  $1300^\circ\text{C}$ , joint temperature measurements of the thermocouple and a two-color pyrometer between  $1300 - 1450^\circ\text{C}$ . Above  $1450^\circ\text{C}$  the molybdenum thermocouple is withdrawn and the pyrometer regulates the furnace alone.

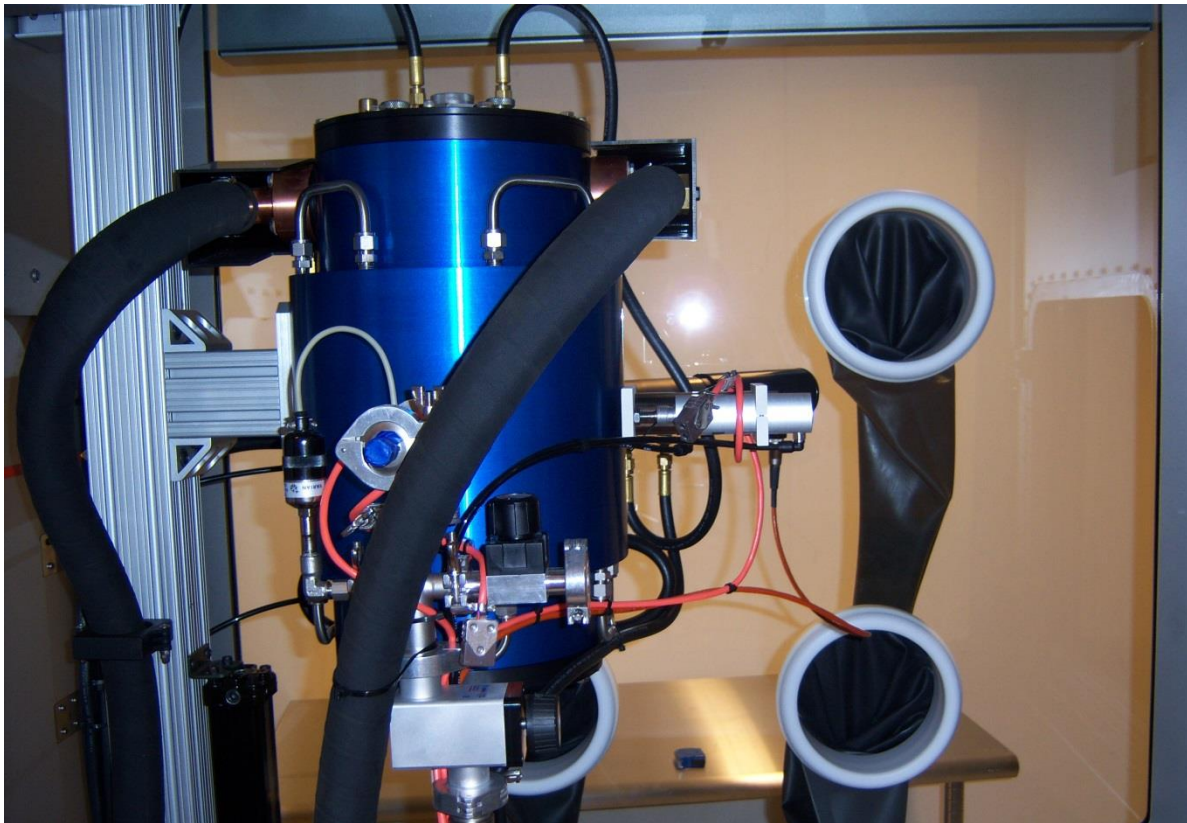


**Figure 4.** High-temperature graphite-heated furnace used for nitridation of produced Zr + C containing microspheres

After insertion of sample in the furnace, it was evacuated and refilled with inert gas. The furnace is placed in a glove box, and when the glove box was in operation and maintained a reasonably pure nitrogen environment (up to maximum around 10 000 ppm of oxygen) the furnace was evacuated and refilled three times in a row to ensure an oxygen-free environment in the furnace. When the atmosphere control of the box was turned off and the box atmosphere was air, the evacuation and refilling of the furnace was performed at least five times to ensure an oxygen-free atmosphere in the furnace. The gases used for nitridation experiments were either nitrogen from the in-house nitrogen gas system (99.996 % N<sub>2</sub>, gas supplier AGA) or nitrogen containing 5 % hydrogen (Air Liquid, gas grade Blue). The material was first heated to 600 °C and held for 2 hours in order to evaporate/break down residues in the microspheres such as urea, HMTA, water and NH<sub>4</sub>NO<sub>3</sub>. The NH<sub>4</sub>NO<sub>3</sub> comes from the washing and ageing step of the microspheres where the NO<sub>3</sub><sup>-</sup> containing microspheres are washed in NH<sub>4</sub>OH (aq).

The microspheres were then heated to between 1400 and 1800 °C and nitriding was performed either in a single step at a temperature in this interval or first at a temperature at the lower end of the range and then a second step at the higher end of the range. The point of or idea behind using two separate heating intervals is to first form the nitride at the lower temperature and burn off the residual carbon through formation of HCN and short-chain hydrocarbons such as CH<sub>4</sub> at the higher temperature step. The higher temperature step is sometimes referred to as the decarburization step.

#### **4.5. Pressing of ZrN pellets and sintering**

Pellets were pressed from produced nitride microspheres using a manual hydraulic press and pressing tools made of tungsten carbide. The pressing die used had a diameter of 9 mm, and the material was pressed without any addition of lubricant. The pressure used was 1.23 GPa. Most of the pellets produced have been pressed from microspheres of a diameter of about 1 mm. This is because there were problems with producing large enough batches of microspheres of reduced size that were sufficiently good in homogeneity and quality to be comparable to each other during nitridation.

Sintering was performed in an N<sub>2</sub> atmosphere, and sintering temperatures used ranged between 1800 – 2000 °C. During sintering the ZrN pellet stood on a molybdenum metal disc in the furnace. The heating rate used during sintering experiments was 10 °C/min and the heat treatment time used at the set temperature was 5 hours.



## 5. Results and Discussion

### 5.1. Carbon stabilization by addition of dispersion agent

In order to increase the settling time, different dispersion agents were tried. Carbon nanotubes are very hydrophobic and will settle quickly if no dispersion aid is used. The carbon particle materials tried as additions to the sols were not equally fast in settling but were still fast enough to require addition of dispersion agents. The nonionic surfactant Triton X-100 was chosen as primary dispersion agent due to the high salt concentration of the system. There are many other nonionic surfactants, but Triton X-100 was chosen due to the fact that it has previously shown the ability to disperse CNTs [RIG 00]. Figure 5 displays the result of leaving a CNT dispersion without any surfactant addition to settle; the settling time for the CNTs was estimated to be on the second scale, in the best case no more than half a minute.

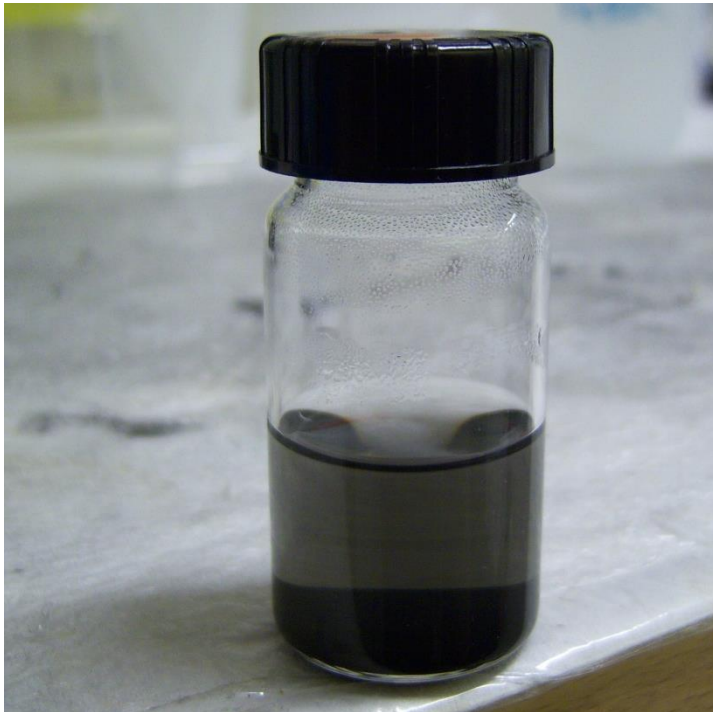


**Figure 5.** Result of trying to disperse CNT in aqueous media without addition of any surfactant.

When Triton X-100 was added to the solution the stability of the dispersions increased strongly for the CNT and the CNP materials. For the coarser carbon powder, however, the stability increase was quite small. This is because the settling time of a dispersion is inversely proportional to the square of the diameter of the dispersed media (solids or droplets) [HOL 03], and when the particles become too large the surface-to-volume ratio becomes too small for any dispersion agent to produce any significant prolongation of the settling time.

Addition of 2 weight-% of Triton X-100 to the aqueous solution greatly increased the suspension stability of both the CNT and the CNP dispersion.



**Figure 6.** Carbon nanotube suspension using Triton X-100 as dispersion agent.

With the use of Triton X-100 as dispersion agent, the resulting particle suspension showed a substantial increase in settling time, and it was regarded as being good enough for use for production of microspheres using the internal sol gel procedure. It has been reported in the literature [RIG 00] that a 5% Triton X-100 solution can produce a good CNT suspension, the reason for using a lower amount of surfactant when producing the sol for the internal sol gel process being to minimize the risk of leakage of water into the silicone oil during the gelation step by transfer of water within micelles formed by the surfactant.

## **5.2. Water leakage into silicone oil**

In order to determine if water to any larger extent was transferred into the silicone oil, a solution of CNT, water and Triton X-100 was prepared and shaken together with the silicone oil (Rhodorsil silicone oil 47). The mixture was left to settle and the silicone oil was separated from the aqueous phase and no trace of water emulsion or CNT could be detected in the oil by visual inspection. Density measurements were performed on the silicone oil that had been mixed with the CNT suspended aqueous phase and compared to density measurements of silicone oil directly taken from its container, the results are presented in Table 2.

**Table 2.** Density measurements on unused silicone oil compared to silicone oil that has been mixed and separated from aqueous solution containing water, Triton X-100 and CNT.

Density mixed silicone oil ( $\text{g}\cdot\text{cm}^{-3}$ )	Density unused silicone oil ( $\text{g}\cdot\text{cm}^{-3}$ )
0.968	0.971
0.968	0.972
0.969	0.973
0.971	0.978
0.969	0.985
Average	Average
0.969	0.9758
Standard deviation	Standard deviation
0.0012	0.0058

No significant different in density could be detected, and together with the visual inspection of the separated silicone oil this was interpreted as indicating that the leakage of aqueous medium into the silicone oil was tolerably small if any.

### 5.3. Gelation of zirconium-containing microspheres

#### 5.3.1. Effect of nozzle vibration

When no vibration of the nozzle was used, the formed microspheres had a size of about 1 mm in diameter when washed and dried. Figures 7 and 8 show produced microspheres as they look just after washing and once they are dried.



**Figure 7.** Picture of produced zirconium + CNT microspheres after washing in petroleum ether and aqueous ammonia and ageing in aqueous ammonia.

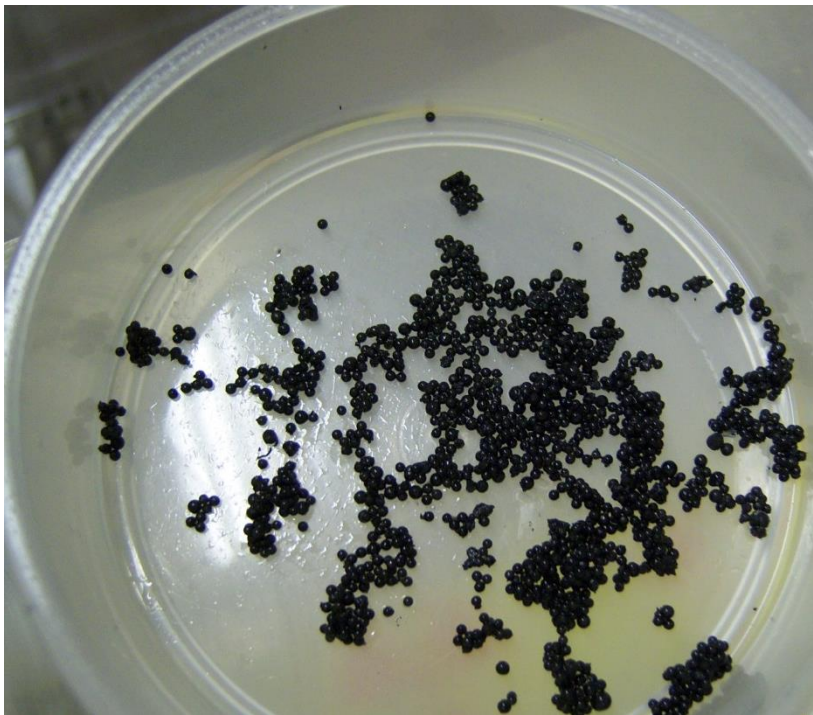


**Figure 8.** Picture of microspheres containing zirconium and CNT after drying.

By applying vibration to the nozzle in the sol gel process, beads smaller than the millimeter-sized ones can be produced. Microspheres down to the range of 50 – 100  $\mu\text{m}$  in diameter have been produced. There is still a problem, however, in obtaining small microspheres with a narrow size distribution. This is partly due to adjusting the sol flow through the nozzle since to rapid flow seeming to cause a slow build-up on the nozzle tip culminating in the formation of larger droplets falling into the gelation column. It was observed that every drop needs a certain amount of time to sink through the silicone oil surface layer. If the droplets hit the surface of the oil too close to each other they will merge and form larger droplets. This is one of the downsides in using an experimental set-up utilizing a stationary gelation column to produce the microspheres. Work that has been performed on the internal sol gel process elsewhere [POU 09] has solved this problem by dripping the sol into a laminar jet stream of silicone oil followed by separation and recirculation of the silicone oil. This type of set-up may have benefits when it comes to production speed capability but requires much more equipment and space for set-up than using a stationary gelation column.

Small microspheres produced by the oscillating nozzle technique can be seen in Figure 9; the microspheres still seem to show good carbon dispersion in the gelled spheres, but the microsphere size distribution can be enhanced.

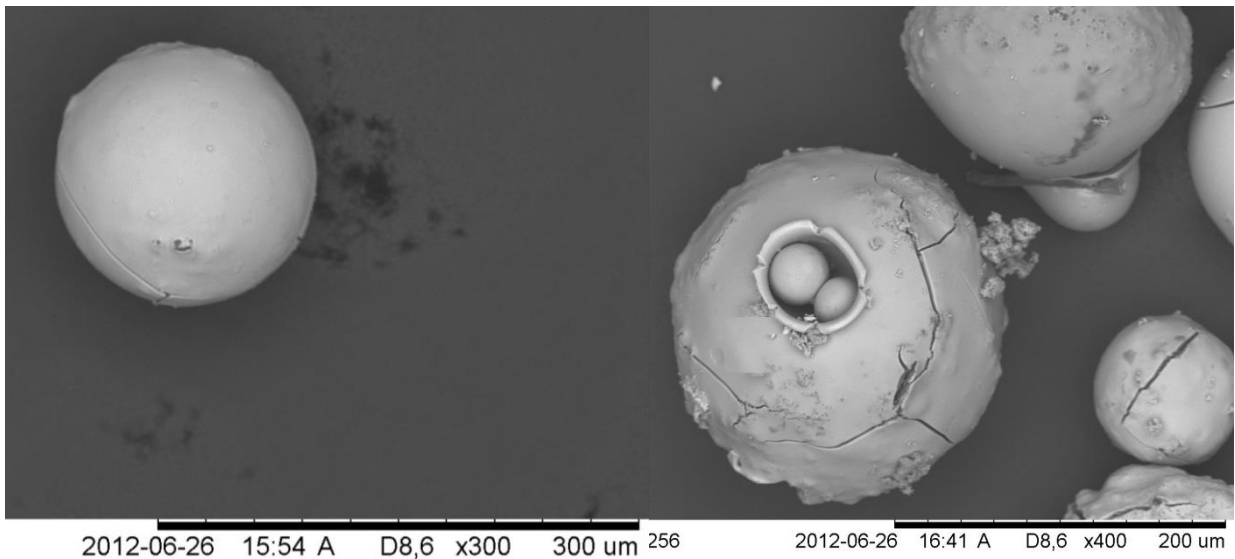


**Figure 9.** Microspheres produced by oscillating nozzle technique. The microspheres do not show any agglomerates of carbon nanotubes, but the internal size variation among the microspheres can be quite large.

### 5.3.2. Effects of carbon addition to the sol

When the coarser carbon powder was used as carbon addition, settling of the powder occurred both in the syringe during gelation and in the droplets during gelation. This resulted in microspheres that displayed a very uneven distribution of the carbon content. As is shown in Figure 10, this uneven carbon distribution could be very clearly detected by SEM characterization of the produced microspheres, especially when smaller microspheres were produced using vibration of the nozzle in the sol gel process.

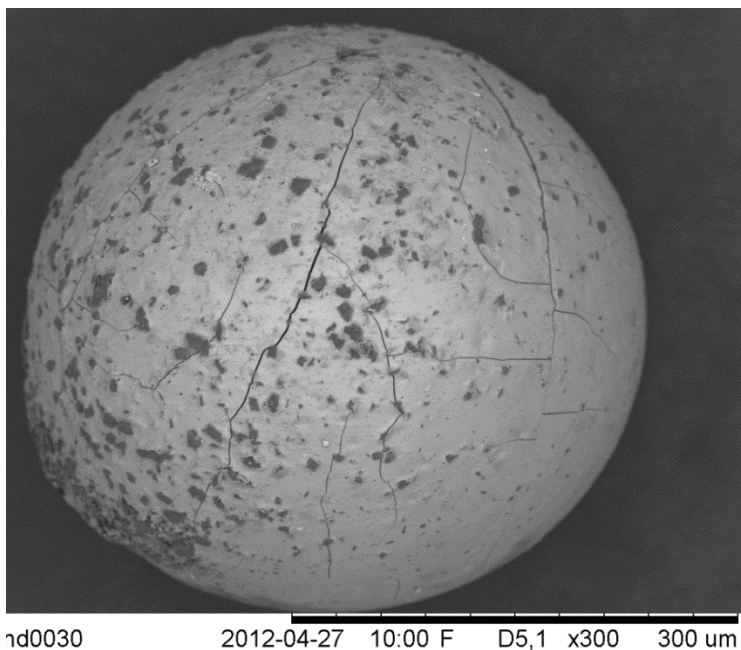


**Figure 10.** Zirconium containing microsphere produced with a coarser graphite powder (about 10 µm size particles). The uneven carbon distribution makes the material impractical for carbothermal reduction.

This result disqualified the graphite powder as a candidate material for producing microspheres suitable for carbothermal reduction since materials with more homogeneous carbon distribution are more favorable for producing nitrides without high concentration clusters of carbon and oxygen remaining in the microspheres.

When CNT or CNP was used as carbon source the resulting microspheres showed a much more homogeneous carbon distribution during SEM characterization, as can be seen in Figure 11.

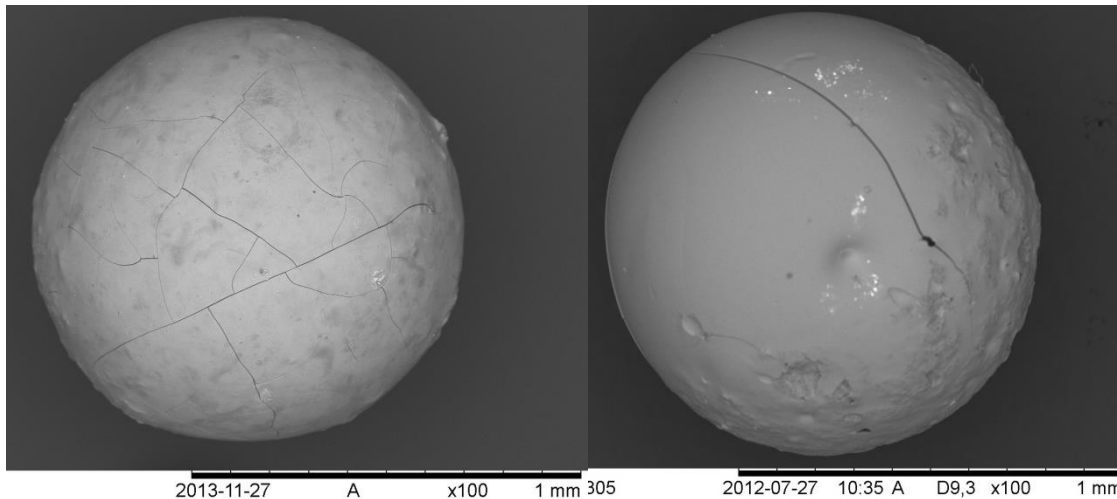


**Figure 11.** To the left microsphere containing CNT and to the right microsphere containing CNP as carbon addition.

#### 5.4. Gelation of uranium containing microspheres

Preparation of ADUN solution was performed, and some gelation studies to find a suitable sol mixture were performed. The ADUN solution was prepared by dissolving  $\text{UO}_2(\text{NO}_3)_2 \cdot 6\text{H}_2\text{O}$  in water and adjusting the  $\text{NO}_3^-/\text{U}$  ratio by addition of  $\text{UO}_3$ . No carbon addition or vibration of the nozzle during gelation was performed on uranium containing sols. Instead several different concentrations of uranium in the sol were tried using the gelation field diagrams produced by Vaidya et.al [VAI 87, VAI 08] as a template for preparation of uranium based microspheres.

The gelation step of the microsphere preparation was in general quite straightforward to perform, and a typical result can be seen in Figure 12.



**Figure 12.** Gelled uranium microspheres produced by internal sol gel technique. Beads have been washed in petroleum ether and ammonium hydroxide and are left for drying.

Several of the examined gelation conditions produce microspheres similar to those seen in Figure 12. The problem encountered, however, comes during washing of the microspheres when they seem to peptize. The result after drying is often quite fragile microspheres which tend to leave quite a lot of dust during handling, Figure 13 shows the microspheres after drying in air at room temperature.



**Figure 13.** The figure shows a typical result after drying the microspheres; a large number of fine particles have fallen off and the microspheres overall are quite prone to mechanical damage.

This peptizing kind of behavior has not been observed in every gelation experiment, however. Experiments starting from a 1.3 M uranium solution produced microspheres that during SEM characterization seemed to avoid any large degree of erosion of material from the microspheres, as can be seen in Figure 14.

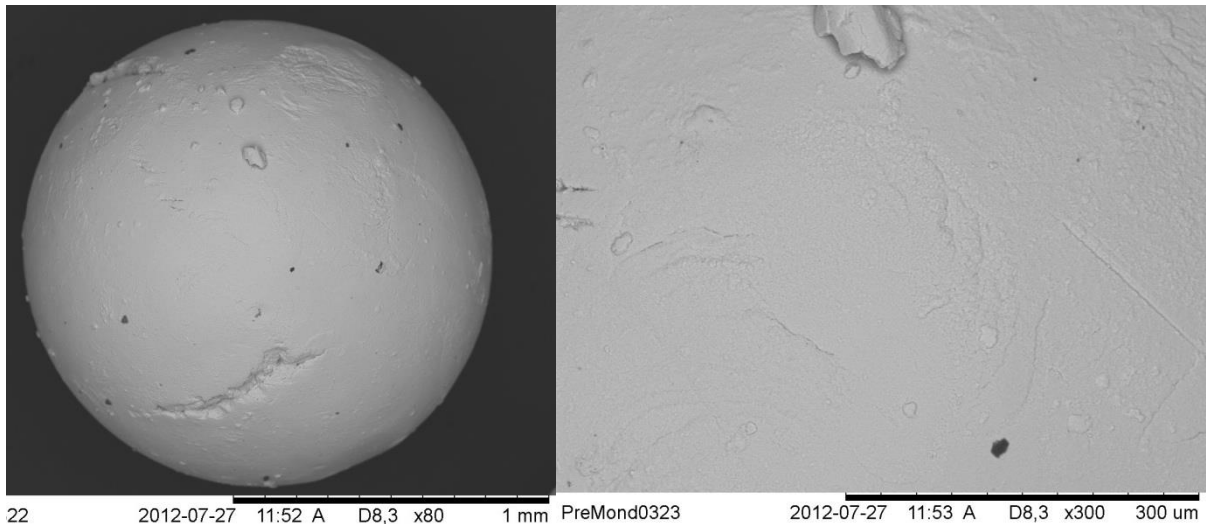


**Figure 14.** Solid uranium microsphere formed from a 1.3 M uranium solution by the internal sol gel technique. The left part of the image presents the entire microsphere while the right image displays a closer examination of the surface structure of the microsphere.

The surface structure of the microsphere depicted in Figure 14 shows a very dense and smooth structure compared to the microspheres in Figure 15, which is an example of how the structure could look in microspheres that eroded during washing.

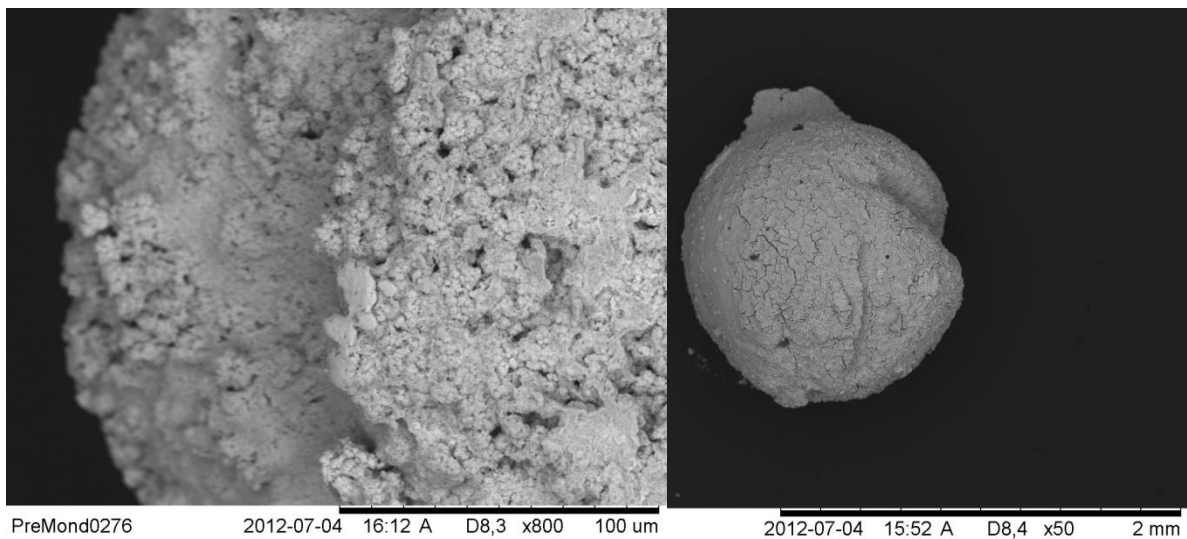


**Figure 15.** Close observations of the microspheres that eroded during washing revealed a much more grainy structure compared to the non-eroding microspheres in Figure 14.

The composition of the sol is not, however, the only thing that affects the outcome of the gelation process. What temperature the sol is kept at when cooled, how long the sol stays in the syringe before being introduced into the silicone oil and what temperature the silicone oil has also affect the outcome. What is generally desired in a sol is that after addition of urea and HMTA it forms a clear solution. If the sol turns opaque during cooling or in the syringe, small light scattering clusters have formed in the sol, and no good gelation results have been observed to date. During gelation the formed microspheres can take on a different color

ranging from bright yellow to orange, depending on what crystallite size and morphology form in the microsphere during gelation. Pale yellow color of the uranium microspheres indicates large crystals sizes and large pores, while a darker, more orange color indicates higher densities and smaller crystals or amorphous structure [COL 04].

### 5.5. Nitriding of zirconium containing microspheres

The result of a nitriding experiment performed on zirconium containing microspheres that was done at 1500 °C can be seen in Figure 16.

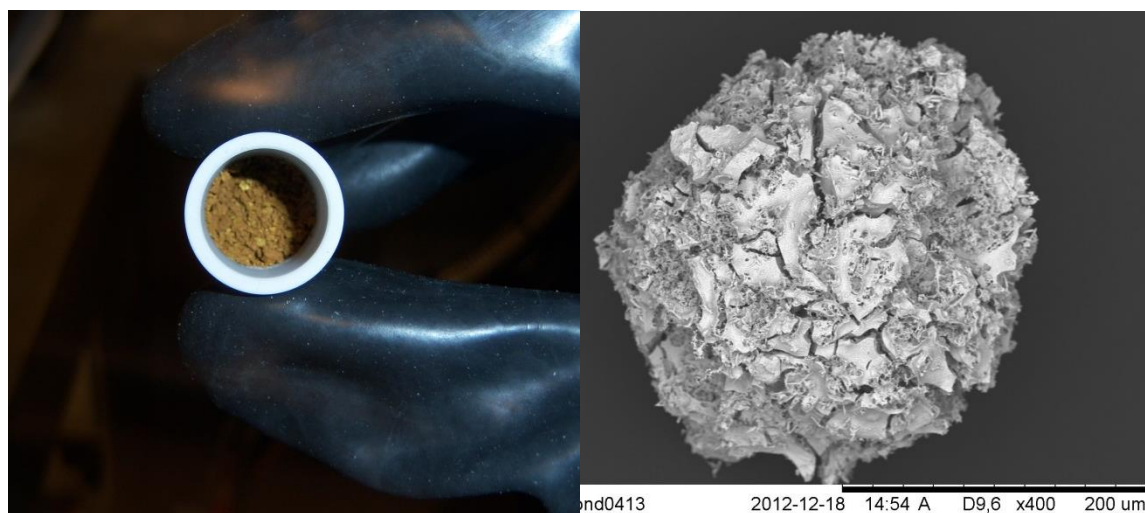


**Figure 16.** Material produced by carbothermal reduction at 1500 °C.

SEM characterization of the material revealed a large degree of porosity and fracturing in the microspheres. This is believed to be caused during the heating step at 600 °C when the residual materials are removed as gas from the microspheres. The heating ramp used was 20 °C per minute, which probably causes the gasification of the residual chemicals to proceed fast enough to cause cracking of the microspheres.

Energy dispersive X-ray spectroscopy (EDX) was used to investigate the elemental composition of the surface of the material, and the results are presented in Table 3.

**Table 3.** Results of EDX measurements performed on the first batch of nitride material.

Element	Series	Composition (at. %)	Uncertainty (%)
Zirconium	L – series	24.3	3.1
Carbon	K – series	51.4	3.5
Nitrogen	K – series	19.0	1.9
Oxygen	K – series	5.2	0.7
Silicon	K – series	0.1	0.0

These results were interpreted as being very strange. According to Table 3 there is about twice as much carbon in the material compared to zirconium. The carbon-to-zirconium ratio in the sol when the material was gelled was 2.3, and for every nitrogen atom added to the

material during nitriding two carbon atoms are removed as CO. Since the nitrogen-to-zirconium ratio is almost 1 according to the EDX measurement, this should mean that there could not possibly be twice as much carbon as zirconium remaining. This could possibly be explained by a surface covering of the microspheres with extra carbon transported there by reactions 13 – 15 from the graphite heating element. This would mean that the surface analysis provided by EDX would produce measurements that do not represent the composition of the bulk material. Another possibility is that the EDX application is simply measuring incorrectly. EDX is known to be less efficient when it comes to quantifying light elements such as carbon, nitrogen and oxygen compared to when measuring heavier elements; for optimal results measurements should also be done on flat smooth surfaces. Quite a large number of EDX measurements have been performed on both dried untreated microspheres and nitride microspheres, and results during measurements have indicated that EDX is a difficult technique to use to obtain good estimates of the elemental composition with respect to the lighter elements present in the materials. An example of this is when measurements have been performed on some nitride samples. The oxygen content measured in these nitrides has been highly dependent on the measurement time. At first the EDX have shown no trace of oxygen up to the point when the EDX has obtained enough data to make a quantification, however if measurements are continued anyway for a short time the EDX will claim the presence of oxygen in the sample. The point where the EDX started observing oxygen also seemed to contain a threshold level, resulting in the registered oxygen level being zero until this point was reached, where it immediately increased to around 3 atomic percent. This kind of stepwise behavior also strengthened the conclusion that EDX could not be used as a reliable tool for quantitative elemental analysis of the produced nitrides.

To be able to make more precise measurements of the elemental composition in the produced nitrides, samples of two different nitridation experiments were taken to an external lab for analysis using high temperature LECO elemental analyzers. N, O and H content was determined by heating the sample in a graphite crucible under an argon atmosphere. The analyzers were calibrated using standards containing known amounts of the elements. The O and H were detected by infrared spectrometry as H<sub>2</sub>O, CO and CO<sub>2</sub>, for determination of nitrogen content, and heat conductivity detectors was used to measure N<sub>2</sub> in the argon stream. One sample of microspheres using CNT as carbon source and one sample containing CNP was brought for analysis and the result is presented in Table 4. The uncertainties in Table 4 are presented as  $\pm 2\sigma$ .

**Table 4.** Results from performed measurements on chemical composition

Sample	Element (weight fraction)				
	O	N	C	H	Zr
Zr + CNT Microspheres	0.356 %	10.5 %	2.96 %	90 ppm	86.2 %
Zr + CNP Microspheres	0.22 ± 0.02%	9.34 ± 0.02%	3.67 %	73 ± 6.4 ppm	86.8 %

It should be noticed that uncertainty is only given for N, O and H content in the Zr + CNP sample. This is because insufficient material was present to perform triplicate measurements on the Zr + CNT sample. When measuring carbon content, sufficient material of the Zr + CNP sample was present to allow duplicate measurement. Therefore no standard deviation could be calculated, but it showed that the measurement data obtained was not totally arbitrary. There was also insufficient material to produce triplicate measurements on the carbon composition of the Zr + CNT sample.

On the assumption that N, O and H are only present in the material as bonded to zirconium and that carbon can be present both as carbide and as free amorphous carbon, an approximate chemical composition is obtained of  $Zr(N_{0.79}C_{0.17}O_{0.024}H_{0.009})$  for the nitride produced by carbothermal reduction with CNT and  $Zr(N_{0.70}C_{0.28}O_{0.014}H_{0.008})$  when CNP was used. These results are considered to be much more credible than the results provided by EDX measurements since they measure the entire sample put into the machine and not just the surface and also because the equipment was calibrated using standards of known composition. It thus seems that it is more of a carbo-nitride than a pure nitride that has formed during the nitridation step.

## 5.6. Sintering of pellets

After pressing and sintering for 5 hours at 2000 °C in an N<sub>2</sub> atmosphere, a nitride pellet typically looks as depicted in Figure 17. The produced pellet displayed what is referred to as a blackberry structure which could also be observed after sintering. A blackberry type of structure is a structure where the individual microspheres do not completely disintegrate during pressing but leave a spherical pattern in the pellet.



**Figure 17.** ZrN pellet sintered for 5 hours at 2000 °C in an N<sub>2</sub> atmosphere.

The yellowish part of the pellet has a color that is usually seen in ZrN, and it was that side that was standing on the molybdenum plate while the red side was exposed to the furnace atmosphere during the sintering step. This result was interpreted as being either the formation of some strange phase on the top of the pellet from impurities in the nitrogen gas used in the furnace or a morphology issue caused by the temperature used.

A new pellet was pressed and sintered in an N<sub>2</sub> atmosphere still using the in-house N<sub>2</sub> system for supplying N<sub>2</sub>, and the sintering temperature was lowered to 1800 °C.

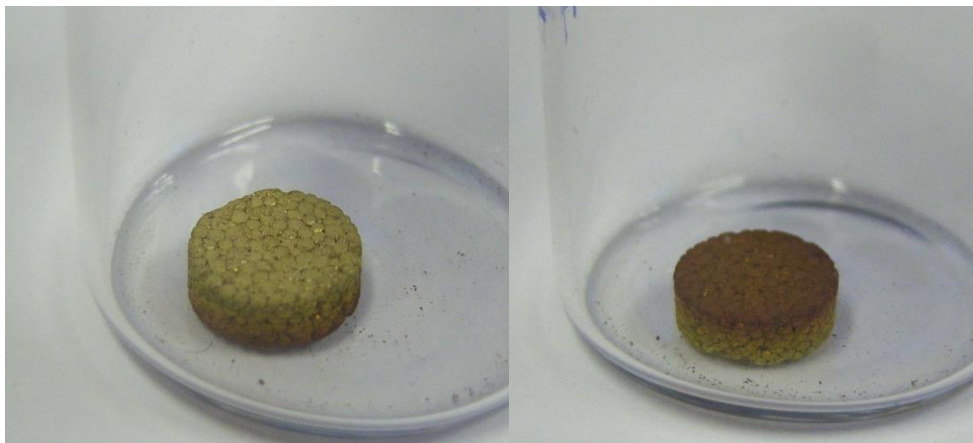


**Figure 18.** ZrN pellet sintered for 5 hours at 1800 °C.

The densification of the pellet was much smaller compared to when sintering at 2000 °C, and it basically retained the physical dimensions it had prior to the sintering step. However, the red on the surface still remained, although less pronounced than in the previous pellet. This behavior led to the conclusion that it was probably not just a temperature phenomenon since nitridations have been carried out up to the same temperature without observations of this red surface. In order to check that there was no impurity in the supplied gas for the furnace another pellet was pressed and sintered at 2000 °C. This time the gas used was high purity N<sub>2</sub> (99.9999 %, Air Liquide) and the flow rate through the furnace was lowered to have as few impurities in the furnace as possible. The result can be seen in Figure 19.

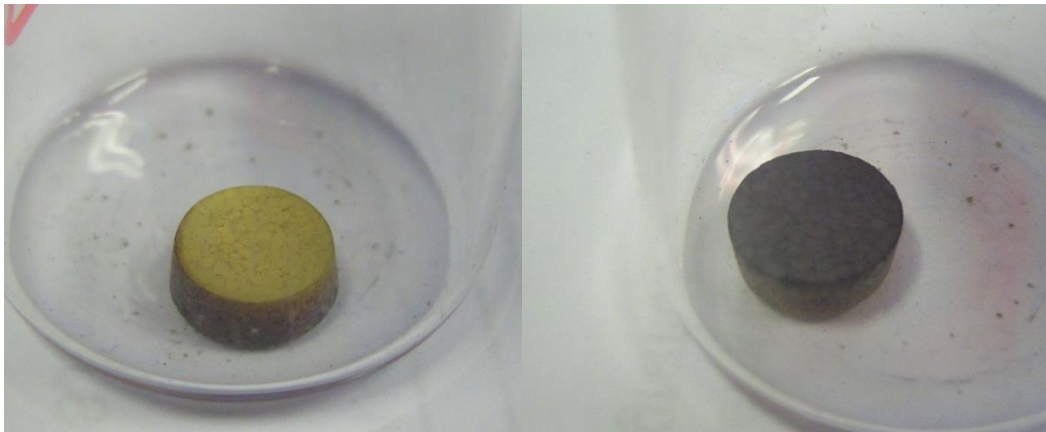


**Figure 19.** Result after 5 h sintering at 2000 °C using 99.9999 % pure N<sub>2</sub> as sintering atmosphere.

This time the top side of the pellet became almost black. This was interpreted as indicating that the problem is not due to the gas used in the furnace but to the furnace itself. The dark phase was believed to be carbon transported as CN compounds from the graphite heating resistor and deposited on the pellet. The reason why a darker phase was obtained on the pellet compared to the pellet in Figure 17 would then be that less carbon from the furnace reaches the pellet but is transported away in the higher gas flow used during that sintering experiment (0.22 dm<sup>3</sup>/min and 0.1 dm<sup>3</sup>/min respectively). SEM and EDX characterizations have been performed on the pellets and the red side of the pellets show higher carbon content than the yellow side. The data from the EDX measurements are presented in Table 5 and is presented as atomic percent. Since EDX has been deemed to be a technique not really suitable for analysis of light elements such as N and C, this was not taken as proof of the hypothesis but rather as an argument for investigating the hypothesis further.

**Table 5.** Results from EDX measurements on the sintered ZrN pellets; the elemental composition is presented as atomic percent.

Sintering condition	Zirconium	Carbon	Nitrogen	Oxygen
2000 °C high purity N <sub>2</sub> yellow side	39.7 ± 3.3	25.9 ± 1.2	34.4 ± 1.8	Not detected
2000 °C high purity N <sub>2</sub> red side	38.4 ± 3.3	34.2 ± 1.5	21.9 ± 1.2	5.5 ± 0.4
2000 °C in house N <sub>2</sub> yellow side	38.9 ± 3.2	23.3 ± 1.2	34.5 ± 1.9	3.4 ± 0.2
2000 °C in house N <sub>2</sub> red side	38.5 ± 3.3	31.4 ± 1.6	21.1 ± 1.3	9.0 ± 0.7
1800 °C in house N <sub>2</sub> yellow side	40.0 ± 3.4	23.1 ± 2.0	36.9 ± 1.2	Not detected
1800 °C in house N <sub>2</sub> red side	37.9 ± 3.4	26.7 ± 1.5	26.2 ± 1.8	9.2 ± 0.8

X-ray diffraction (XRD) was performed on both the yellow and red sides of the pellet sintered in high purity N<sub>2</sub>, and the diffractogram is presented in Figure 20.

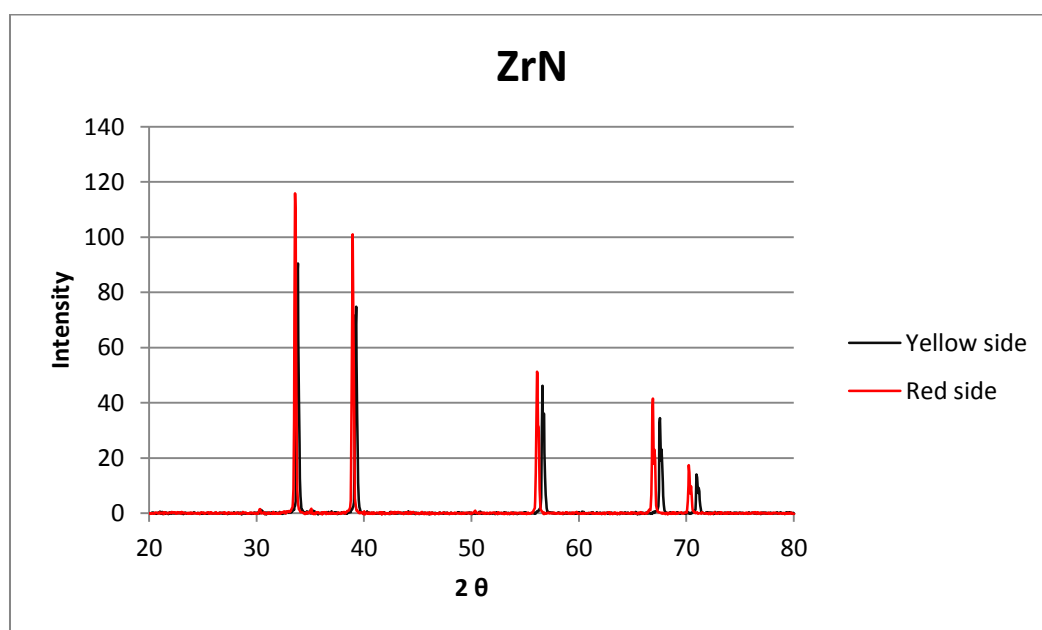


**Figure 20.** Diffractograms for both the red and the yellow side of the pellet sintered in high purity N<sub>2</sub>.

The extended angle XRD measurements up to  $150^\circ 2\theta$  for the ZrN sintered in high purity  $N_2$  are presented in Appendix I. From these data the lattice constant for the yellow side is calculated to be  $4.598 \pm 9.4 \cdot 10^{-4} \text{ \AA}$  and for the red side  $4.644 \pm 1.00 \cdot 10^{-2} \text{ \AA}$ . The tabled lattice parameter for sub-stoichiometric zirconium nitride ( $ZrN_{0.93}$ ) is  $4.5755 \text{ \AA}$  [HEL 78] and theoretically calculated for ZrN is  $4.59 \text{ \AA}$  [SAH 10]. The lattice constant for ZrC is  $4.698 \text{ \AA}$  [KEM 60]. Since both ZrN and ZrC adopt NaCl-fcc crystal structure, the mixture in a solid solution of these two compounds will have a lattice parameter between the two of the pure substances, and the red side shows a larger shift towards the carbide lattice constant than the yellow side. It is thus reasonable to assume that if the red side of the pellet contains a larger amount of carbide than the yellow side, it must have formed during sintering, and this would indicate transportation of carbon from the furnace to the surface of the pellet. If it is assumed that the system studied can be regarded as being a binary solid solution between ZrN and ZrC, Vegard's law predicts that the yellow side of the pellet, i.e. the side that has not been in direct contact with the sintering atmosphere, would have the composition  $Zr(N_{0.82}C_{0.18})$ . The sintered pellet in Figure 19 was pressed from the same batch material as the Zr + CNT sample measured for C, N, O and H content in Table 4. Thus the result obtained by XRD agrees well with the structure estimated by elemental analysis. The application of Vegard's law to the red side of the pellet, assuming it consists of carbide and nitride, predicted a structure of  $Zr(N_{0.45}C_{0.55})$ . These results should be interpreted very cautiously, however, partly since the calculation predicts a more or less 50 – 50 composition which is in the region where the uncertainties connected to the use of Vegard's law ought to be greatest [JAC 07]. Another reason for caution is that the data evaluation suggested that the red side could contain Zr(C, O) or ternary Zr(N, C, O) structures. Vegard's law treats binary solid solutions; therefore it is thus not really possible to estimate the compositions of a three-component system since several different N, C and O combinations could produce very similar shifts in the diffractogram.

Closer investigations of the blackberry structures formed in the pellets pressed were performed using SEM imaging. The surface structure of the pellet sintered at  $2000^\circ\text{C}$  under in-house  $N_2$  gas is shown in Figures 21 and 22.

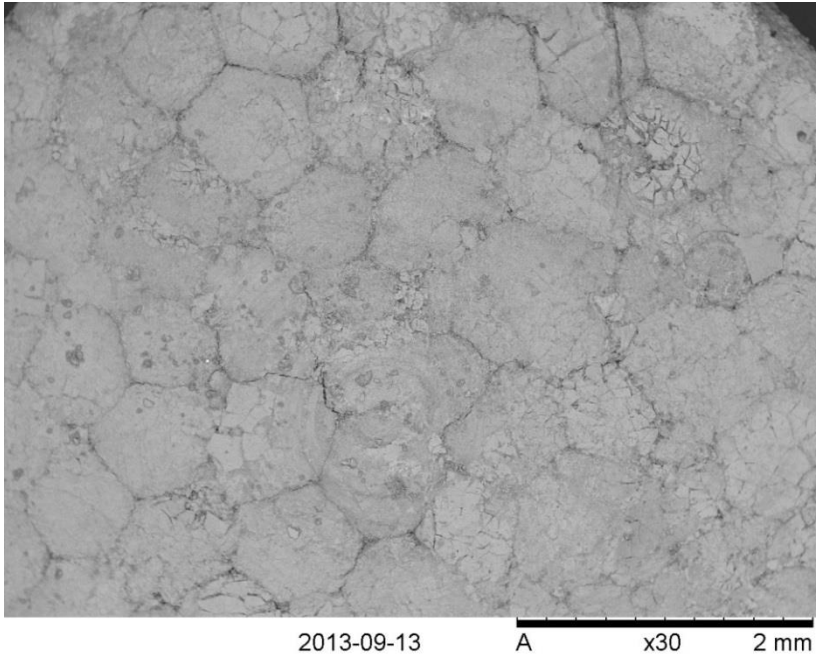


**Figure 21.** Blackberry structure of the pressed and sintered pellet.

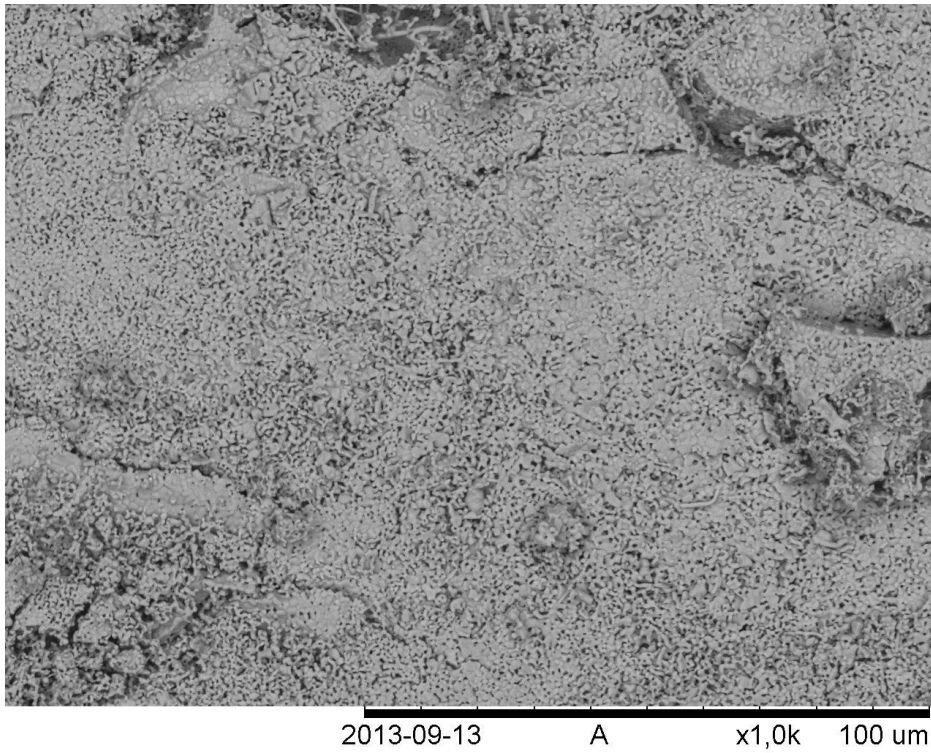


**Figure 22.** Microstructure on the surface of the sintered pellet.

Figures 21 and 22 are images produced by analysis of the surface of the pellet that had been on the molybdenum plate during sintering. Investigations of the top of the pellet revealed a surface structure that appeared to be identical to the structure of the bottom, so imaging of that side is omitted. Figure 21 reveals clear boundaries between the individual microspheres. This behavior indicates that the sintering step has not been able to fuse the individual microspheres properly and represents an unwanted structure since it will be a rather difficult task to produce pellets of high density if the microspheres cannot be sintered together properly. This kind of structure will also probably have an adverse impact on properties such as thermal conductivity and fission gas retention. It will probably be necessary to greatly reduce the size of the microspheres in order to reduce the average boundary distance between the microspheres. An option would be if the nitride microspheres could be produced with sufficiently low crush strength to completely disintegrate during pressing. However, there would still be a problem with packing the microspheres closely in the pressing die if using mm-sized spheres. Figure 22 reveals that the surface is filled with small pores distributed across the surface of the pellet. In Figure 23 it can be seen that the pores in Figure 22 are of the order of about 1  $\mu\text{m}$  and there appear to be absences of individual grains in the structure.

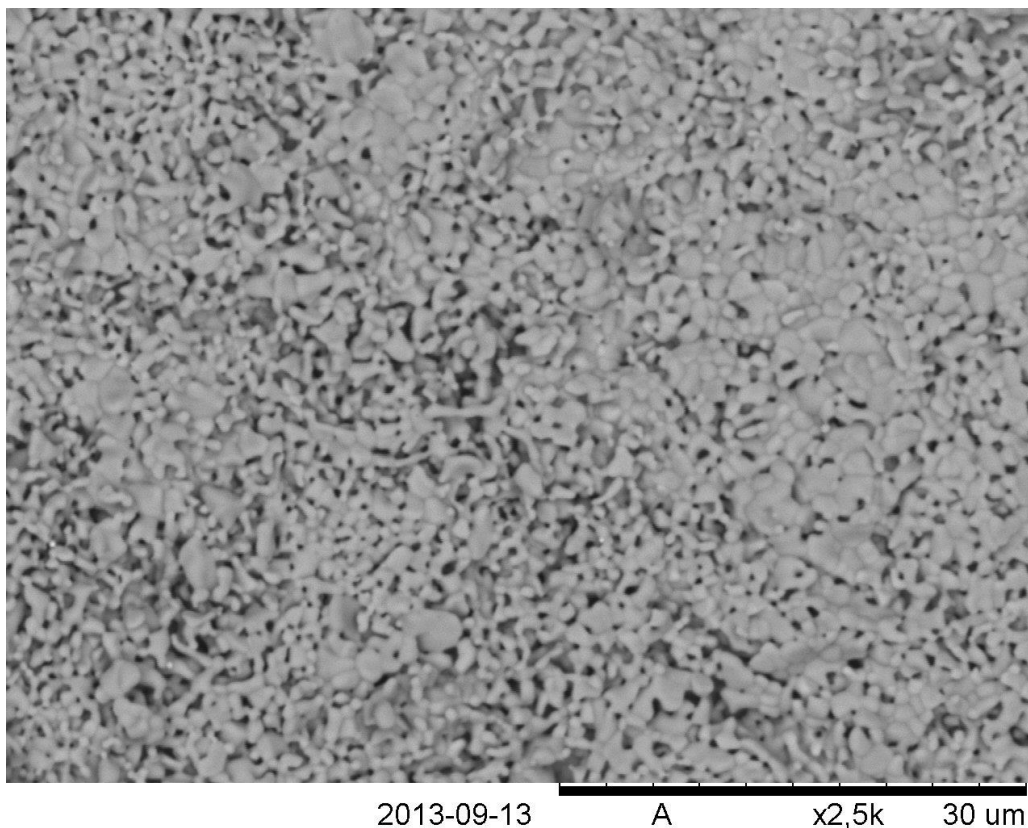


**Figure 23.** Open porosity of  $\mu\text{m}$  scale could be detected on the surface of the pellet.

The reason for this structure can hardly be explained by the size of the microspheres used. Possible reasons could be that the nitridation reaction has not reached completion and that additional nitride has formed during sintering. If this is the case, additional CO gas has evolved in the pellet while sintering and outflow of gas from the pellet may inhibit the sintering process.

The result of sintering at 1800 °C is presented in Figure 24.

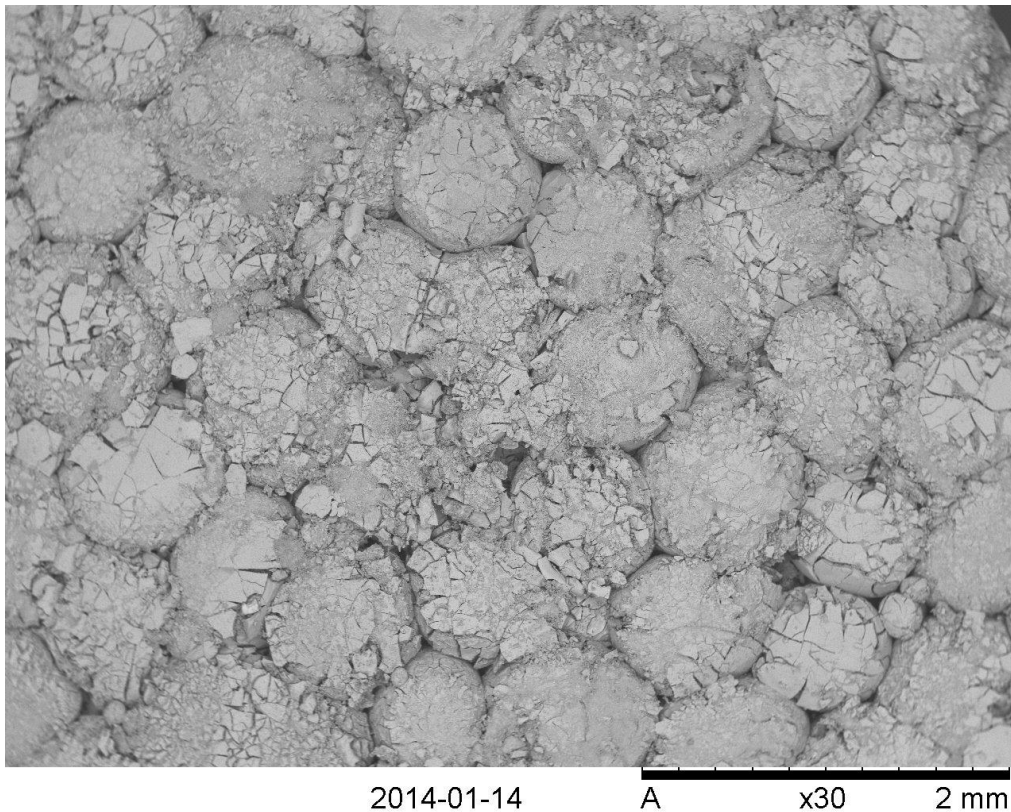


**Figure 24.** Examination of the pellet surface revealed a structure that appears to hardly have sintered at all.

The pellet does not seem to have sintered to any large degree at all. It does, however, show that there is a significant difference between sintering at 1800 °C and 2000 °C. 2000 °C is a quite high sintering temperature, and 1800 °C is closer to sintering temperatures encountered in the literature (1750 °C,  $(Zr_{0.8},U_{0.2})N$  material) [BUR 01], where it appears to have been applied successfully. The reason for the less efficient sintering observed during these experiments is most likely that powders have been used in the literature encountered. Pressing from powders will effectively minimize the sizes of the pores present in the material prior to sintering and thereby also greatly reduce the diffusion distances. It is, of course, difficult to make a direct comparison with a published paper where 20% uranium has been present in the nitride material, although when looking at the neck growth that has occurred between the microspheres in Figure 24 the argument still holds since it is clear that some consolidation of the microspheres has occurred. The result of the 1800 °C sintering should therefore not be interpreted as proof that sintering at this temperature would be insufficient, but rather as an indication that size reduction of the microspheres used during pelletization is necessary in order to produce good-quality pellets.

## 6. Conclusions

Sol gel-derived microspheres containing zirconium and carbon as a precursor material for ZrN formation have been produced. Different carbon additions were tested for suitability as carbon sources during the internal sol gel process, and the use of Triton X-100 as dispersion agent has so far appeared successful. The size of the microspheres produced can be affected by nozzle vibrations, however further optimization to improve size homogeneity is required. The purity reached of produced nitrides has been determined to be in the range of about  $Zr(N_{0.7}C_{0.3})$  to  $Zr(N_{0.8}C_{0.2})$  with some additional carbon remaining as elemental carbon and also some residual oxygen contamination. It is difficult to draw any definitive conclusion about the oxygen level measured since microspheres were stored in air for extended time periods prior to measuring. The residual level of carbon suggests that the C/Zr ratio of 2.3 used during nitridation experiments could be lowered to some degree in order to reduce the carbon content in the final product.

Sintering of nitride pellets at high temperatures in  $N_2$  produced a reddish surface on the pellet surface facing the sintering atmosphere. XRD characterization suggests this surface being covered with either carbo-nitride, oxy-carbide or a ternary  $Zr(N, O, C)$  composition. The surface of the pellet on the molybdenum plate during sintering seems to be unaffected in chemical composition by the heat treatment.

Sintering performed at 2000 °C produced a clear sintering effect compared to sintering at 1800 °C, although neck growth also occurred to a limited degree at this temperature. The sintered pellets displayed quite pronounced boundaries between individual microspheres in the blackberry structure even when sintering at 2000 °C. This suggests that a reduction in the size of the microspheres may be beneficial in order to achieve less space between the individual microspheres and improve sintering. Another option would be production of microspheres with sufficiently low crush strength to disintegrate during pelletization.



## 7. Future work

Continuation of this work will include further optimization of the size and size distribution control of microspheres produced by the internal sol gel technique.

Another feature to be investigated is the nitride purity and pelletization properties as a function of microsphere size during specified process conditions.

Sintering studies will be continued, investigating densification behavior depending on microsphere size, crushability during pressing and sintering atmosphere.

Introduction of plutonium into the sol gel feed broth for the production and characterization of (Zr, Pu)N fuel pellets.

Since no detailed chemistry could be found in the literature regarding internal sol gel with only plutonium as metallic specie present in the sol it would be interesting to study these types of systems.

It may perhaps also be possible to investigate the thermal conductivities of fuel pellets produced by the internal sol gel technique and study the influence of not only density but also internal pellet morphology on thermal conductivity.

If possible it would also be interesting to examine the sintering properties of ZrN pellets pressed from microspheres by spark plasma sintering.



## 8. Acknowledgements

There are several people I would like to thank who have all helped me along the way to this thesis.

I would like to express my thanks to my supervisor Christian, for making this project a reality in the first place, for all the help given during scientific discussions, for incredible speed in answering e-mails regardless of the time or the irrelevance of my questions and for guiding me like a Virgil down the path of Infer... I mean statistics.

To Gunnar, for endless help with setting up the fuel lab, for always taking time to answer my questions and for all enlightening talks about matters both big and small.

To Britt-Marie for help with evaluation of XRD data.

I am also grateful to Sven-Erik Bäckman for help with elemental analysis and for allowing me to come to Degerfors and for teaching me the measurement methods.

To Emma & Elin for taking me into your office and for all the help you gave me when I was new and confused about just enough everything.

Special thanks are due to Lovisa for help with the sol gel work and for being excellent company during travel to conferences and courses no matter how lost or hungry we became before we found our way.

To each and every one of you at the department for making it such fun to go to work.

To my family for never-ending support and care.

Finally to Emma, just for being you, for being part of my life, for making me a better person and for meaning more to me than I could possibly express in words.

The research leading to these results has received funding from the European Atomic Energy Community's Seventh Framework Programme FP7/2007-2011 under grant agreement n°295825



## 9. Bibliography

- [ADA 85] Adamson, M.G., Aitken, E.A., Caputi, R.W., *Experimental and thermodynamic evaluation of the melting behavior of irradiated oxide fuels*, 1985, Journal of Nuclear Materials 130, pp. 349 – 365
- [ALL 67] Allbutt, M., Dell, R.M., *Chemical aspects of nitride, phosphide and sulphide fuels*, 1967, Journal of Nuclear Materials 24, pp. 1-20
- [APA 12] Aparicio. M., Jitianu. A., Klein. L.C., *Sol-Gel Processing for Conventional and Alternative Energy*, pp. 341 – 373, New York, Springer Science + Business media, 2012
- [ARA 98] Arai, Y., Nakajima, K., Suzuki, Y., *Thermal conductivity of actinide mononitride solid solutions*, 1998, Journal of alloys and compounds 271-273, pp. 602-605
- [BAR 92] Bardelle, P., Warin, D., *Mechanism and kinetics of the uranium-plutonium mononitride synthesis*, 1992, Journal of Nuclear Materials 188, pp. 36-42
- [BAR 08] Bart, G., Botta, F.B., Hoth C.W., Ledergerber, G., Mason, R.E., Stratton, R.W., *AC-3-irradiation test of sphere – pac and pellet (U,Pu)C fuel in the US Fast Flux Test Facility*, 2008, Journal of Nuclear Materials 376, pp. 47 – 59
- [BEG 90] Begun, G.M., Haire, R.G., *Raman spectra of some actinide dioxides and of EuF<sub>2</sub>*, 1990, Journal of the Less-Common Materials 162, pp. 129 – 133
- [BEN 69] Benz, R., *Melting Point Maxima of ThC – ThN and of UC – UN Solid Solutions*, 1969, Journal of Nuclear Materials 31, pp. 93 – 98
- [BEN 70] Benz, R., Hutchinson, W.B., *U + N<sub>2</sub> reaction layer growths*, 1970, Journal of Nuclear Materials 36 (2), pp. 135 – 146
- [BEN 08] Beany, G., *Fabrication of Zirconia based ceramics by internal gelation for conversion of trivalent actinides*, PhD-thesis Forschungszentrums Jülich, 2008
- [BER 89] Bernard, H., *Advanced fuel fabrication*, 1989, Journal of Nuclear Materials 166, pp. 105 – 111
- [BLA 88] Blank, H., *Specification and Characterization of Dense Fuels for Liquid Metal Cooled Fast Breeder Reactors*, 1988, Journal of Nuclear Materials 153, pp. 171 – 177
- [BLA 89] Blank, H., Richter, K., Coquerelle, M, Matzke, Hj., Campana, M., Sari, C., Ray, I.L.F., *Dense fuels in Europe*, 1989, Journal of Nuclear Materials 166, pp. 95 – 104
- [BRU 70] Bruggen v.d, F.W., Noothout, A.J., Hermans, M.E.A., Kanij., J.B.W., Votocek, O., *a U(VI) – process for microsphere production*, 1970, Symposium on sol-gel processes and reactor fuel cycles. Gatlinburg, Tennessee, CONF – 700502, pp. 253 – 263
- [BRY 14] Brykala, M., Deptula, A., Rogowski, M., Lada, W., Olczak, T., Wawaczak, D., Smolinski, T., Wojtowicz, P., Modolo, G., *Synthesis of microspheres of triuranium octaoxide*

by simultaneous water and nitrate extraction from ascorbate-uranyl sols, 2014, Journal of Radioanalytical Nuclear Chemistry, pp. 651 – 655

[BUR 01] Burghartz, M., Ledergerber, G., Hein, H., Laan v.d, R.R., Konings, R.J.M., *Some aspects of the use of ZrN as an inert matrix for actinide fuels*, 2001, Journal of Nuclear Materials 288, pp. 233 – 236

[CHA 08] Charollais, F., Perrais, C., Moulinier, D., Perez, M., Vitali, M.P., *Latest achievements of CEA and AREVA NP on HTR fuel fabrication*, 2008, Nuclear Engineering and Design 238, pp. 2854 – 2860

[CHO 02] Choppin, G., Liljenzin, J.O., Rydberg, J., *Radiochemistry and nuclear chemistry, third edition*, Woburn (U.S), Butterworth-Heinemann, 2002

[CIR 09] Ciriello, A., Rondinella, V.V., Staicu, D., Somers, J., Benes, O., Jardin, R., Bouëxière, D., Wastin, F., Colineau, E., *Thermophysical characterization of ZrN and (Zr,Pu)N*, 2009, Journal of alloys and compounds 473, pp. 265-271

[COL 87] Collins, J.L., Lloyd, M.H., Fellows, R.L., *The Basic Chemistry Involved in the Internal-Gelation Method of Precipitating Uranium as Determined by pH Measurements*, 1987, Radiochimica Acta 42, pp. 121-134

[COL 04] Collins, J.L., Hunt, R.D., Del Cul G.D., Williams, D.F., *Production of depleted UO<sub>2</sub> kernels for the advanced gas-cooled reactor program for use in Triso coating development*, 2004, ORNL/TM-2004/123

[FU 04] Fu, X., Liang, T., Tang, Y., Xu, Z., Tang, C., *Preparation of UO<sub>2</sub> Kernel for HTR-10 Fuel Element*, 2004, Journal of Nuclear Science and Technology 41 (9), pp. 943 – 948

[GAN 91] Ganguly, C., Hegde, P.V., Sengupta, A.K., *Preparation and characterisation and out-of-pile property evaluation of (U, Pu)N fuel pellets*, 1991, Journal of Nuclear Materials 178, pp. 234-241

[GAN 93] Ganguly, C., *Sol – gel microsphere pelletization: A powder – free advanced process for fabrication of ceramic nuclear fuel pellets*, 1993, Bulletin of Material Science 16 (6), pp. 509 – 522

[GAN 97] Ganguly, C., Hedge, P.V., *Sol – Gel Microsphere Pelletization Process for Fabrication of (U, Pu)O<sub>2</sub>, (U, Pu)C and (U, Pu)N Fuel Pellets for the Prototype Fast Breeder Reactor in India*, 1997, Journal of Sol – Gel Science and Technology 9, pp. 285 – 294

[GIB 71] Gibby, R.L., *The effect of plutonium content on the thermal conductivity of (U, Pu)O<sub>2</sub> solid solutions*, 1971, Journal of Nuclear Materials 38, pp. 163 – 177

[HAG 04] Hagfeldt, C., Kessler, V., Persson, I., *Structure of the hydrated, hydrolysed, and solvated zirconium (IV) and hafnium (IV) ions in water and aprotic oxygen donor solvents. A crystallographic, EXAFS spectroscopic and large angle X-ray scattering study*, 2004, Dalton Transactions 14, pp. 2142 – 2151

- [HAY 90a] Hayes, S.L., Thomas, J.K., Peddicord, K.L., *Material property correlations for uranium mononitride IV. Thermodynamic properties*, 1990, Journal of Nuclear Materials 171, pp. 300-318
- [HAY 90b] Hayes, S.L., Thomas, J.K., Peddicord, K.L., *Material property correlations for uranium mononitride I. Physical properties*, 1990, Journal of Nuclear materials 171, pp. 262-270
- [HAY 12] Haynes, W.M., ed, “ *Properties of the elements and inorganic compounds* ” in *CRC Handbook of Chemistry and Physics, 92<sup>nd</sup> edition Internet version 2012*, CRC Press/Taylor and Francis, Boca Raton, FL, 2012
- [HEL 78] Hellwege, K.-H., Crystal structure data of inorganic compounds. In *Landolt - Börnstein Numerical Data and Functional Relationships in Science and Technology*, 1978,  
[http://www.springermaterials.com/docs/pdf/10201501\\_10.html?queryterms=%22zrn%22](http://www.springermaterials.com/docs/pdf/10201501_10.html?queryterms=%22zrn%22),  
 (2014-01-10)
- [HOL 68] Holleck, H., Smailos, E., Thümmeler, F., *Zur Mischallkristallbildung in den quasibinären Systemen von UN und den Mononitriden der IV A-Gruppe TiN, ZrN und HfN*, 1968, Monatshefte für Chemie 99, pp. 985-989
- [HOL 03] Holmberg, K., Jönsson, B., Kronberg, B., Lindman, B., *Surfactants and polymers in aqueous solution 2<sup>nd</sup> edition*, Chichester, John Wiley & sons Ltd, 2003
- [HUN 10] Hunt, R.D., Montgomery, F.C., Collins, J.L., *Treatment techniques to prevent cracking of amorphous microspheres made by internal gelation process*, 2010, Journal of Nuclear Materials 405, pp. 160 – 164
- [IAE 13] IAEA, *Nuclear Technology Review 2013*, Vienna, Printed by the IAEA, 2013
- [ISL 03] Islam, M.F., Rojas, E., Bergey, D.M., Johnson, A.T., Yodh, A.G., *High Weight Fraction Surfactant Solubilization of Single – Wall Carbon Nanotubes in Water*, 2003, Nano Letters 3 (2), pp. 269 – 273
- [JAC 07] Jacob, K.T., *Vegard’s law: a fundamental relation or an approximation?*, 2007, International Journal of Materials Research 98 (9), pp. 776 – 779
- [JCP 13] JCPDS – International Center for Diffraction Data, PDF – 4+, (2013), 12 Campus Blvd., Newton Square, PA 19073 – 3273 U.S.A.
- [KAN 74] Kanij, J.B.W., Noothout, A.J., Votocek, O., *The KEMA U(VI)-Process for the Production of UO<sub>2</sub> Microspheres*, 1974, in Sol-Gel Process for Fuel Fabrication. IAEA-161, pp. 185 – 195
- [KEM 60] Kempter, C.P., Fries, R.J., *189. Zirconium Carbide*, 1960, Analytical Chemistry 32 (4), pp. 570

- [KIN 90] King, C.M., King, R.B., Garber, A.R., Thompson, M.C., Buchanan, B.R., *Magnetic Resonance as a Structural Probe of a Uranium (VI) Sol-Gel Process (U)*, 1990, Materials Research Society: Better Ceramics Through Chemistry IV Symposium
- [KLE 99] Kleykamp, H., *Selection of materials as diluents for burning of plutonium fuels in nuclear reactors*, 1999, Journal of Nuclear Materials 275, pp. 1-11
- [LED 92] Ledergerber, G., Kopajtic, Z., Ingold, F., Stratton, R.W., *Preparation of uranium nitride in the form of microspheres*, 1992, Journal of Nuclear Materials 188, pp. 28-35
- [LED 96] Ledergerber, G., *JAERI Review - Internal Gelation for Oxide and Nitride Particles*, 1996, Japan Atomic Energy Research Institute
- [LLO 76] Lloyd, M.H., Bischoff, K., Peng, K., Nissen, H-U., Wessicken, R., *Crystal Habit and Phase Attribution of U(VI) Oxides in a Gelation Process*, 1976, Journal of inorganic nuclear Chemistry 38, pp. 1141 – 1147
- [LLO 78] Lloyd, M.H., Haire, R.G., *The Chemistry of Plutonium in Sol-Gel Processes*, 1978, Radiochimica Acta 25, pp. 139 – 148
- [MAT 86] Matzke, Hj., *Science of Advanced LMFBR Fuels*, Amsterdam, Elsevier Science Publishers, 1986
- [MAT 91] Matzke, Hj., *Fabrication and Testing of Non – Oxide Nuclear Fuels for Fast Breeders*, 1991, Ceramics International 17, pp. 315 – 323
- [MUK 90] Mukerjee, S.K., Dehadraya, J.V., Vaidya, V.N. Sood, D.D., *Kinetic study of the carbothermic synthesis of uranium monocarbide microspheres*, 1990, Journal of Nuclear Materials 172, pp. 37-46
- [MUK 91] Mukerjee, S.K., Dehadraya, J.V., Vaidya, V.N., Sood, D.D., *Kinetics of the carbothermic synthesis of uranium mononitride microspheres*, 1991, Journal of Nuclear Materials 185, pp. 39-49
- [MUK 93] Mukerjee, S.K., Rama Rao, G.A., Dehadraya, J.V., Vaidya, V.N., Venugopal, V., Sood, D.D., *Carbothermic reduction of (UO<sub>3</sub> + C) microspheres to (UO<sub>2</sub> + C) microspheres*, 1993, Journal of Nuclear Materials 199, pp. 247-257
- [MUR 77] Muromura, T., Tagawa, H., *Formation of uranium mononitride by the reaction of uranium dioxide with carbon in ammonia and a mixture of hydrogen and nitrogen – I synthesis of high purity UN*, 1977, Journal of Nuclear Materials 71, pp. 65-72
- [OET 67] Oetting, F.L., *The chemical thermodynamic properties of plutonium compounds*, 1967, Chemical Reviews 67 (3), pp. 261 – 297
- [OI 72] Oi, N., Hirayama, S., Tanabe, I., Muramatsu, A., Kawada, T., *Preparation of High Density Uranium Nitride and Uranium Carbonitride Fuel Pellets*, 1972, Journal of Nuclear Science and Technology 9 (9), pp. 521 – 527

- [OET 78] Oetting, F.L., *The chemical thermodynamic properties of nuclear materials III. Plutonium mononitride*, 1978, Journal of Chemical thermodynamics 10, pp. 941 – 948
- [OLS 63] Olson, W.M., Mulford, R.N.R., *The decomposition pressure and meltingpoint of uranium mononitride*, 1963, Journal of physical chemistry 67 (4), pp. 952 – 954
- [OLS 64] Olson, W.M., Mulford, R.N.R., *The decomposition pressure of plutonium nitride*, 1964, Journal of Physical Chemistry 68 (5), pp. 1048 – 1051
- [PAU 88] Pautasso, G., Richter, K., Sari, C., *Investigation of the reaction  $UO_{2+x} + PuO_2 + C + N_2$  by thermogravimetry*, 1988, Journal of Nuclear Materials 158, pp. 12-18
- [PAR 11] Parkison, A.J., McDeavitt, S.M., *Hydride Formation Process for the Powder Metallurgical Recycle of Zircaloy from Used Nuclear Fuel*, 2011, Metallurgical and Material Transactions A: Physical Metallurgy and Materials Science 42 (1), pp. 192-201
- [PIA 91] Pialoux, A., Achour, M., *Diffraction de Rayons X à haute température et réactivité chimique: application à la nitruration carbothermique de la zircone*, 1991, Journal of the Less-Common Materials 169, pp. 317 – 330
- [POP 00] Popov, S.G., Ivanov, V.K., Carbajo, J.J., Yoder, G.L., *Thermophysical properties of MOX and UO<sub>2</sub> fuels including the effects of irradiation*, 2000, ORNL/TM-2000/351
- [POU 09] Pouchon, M.A., Ingold, F., *Internal Gelation at PSI: The past and the future*, 2009, Proceedings of ICAPP 09, paper 9494
- [RAH 03] Rahaman, M.N., *Ceramic Processing and Sintering 2<sup>nd</sup> edition*, New York, Marcel Dekkers, 2003
- [RAM 91] Rama Rao, G.A., Mukerjee, S.k., Vaidya, V.N., Venugopal, V., Sood, V.V., *Oxidation and hydrolysis kinetic studies on UN*, 1991, Journal of Nuclear Materials 185, pp. 231 – 241
- [RIE 11] Riedel, R., Chen, I-W., *Ceramics Science and Technology, Volume 3 : Synthesis and Processing*, Hoboken NJ USA, Wiley, 2011
- [RIG 00] Riggs, J.E., Walker, D.B., Carroll, D.L., Sun, Y.P., *Optical Limiting Properties of Suspended and Solubilized Carbon Nanotubes*, 2000, Journal of Physical Chemistry, pp. 7071 – 7076
- [ROG 11] Rogozkin, B.D., Stepenova, N.M., Fedorov, Y.E., Shishkov, M.G., Kryukov, F.N., Kuzmin, S.V., Nikitin, O.N., Kurina, I.S., Zabudko, L.M., Noirot, J., Bejaoui, S., *Post-Reactor Studies of Plutonium Mononitride and Oxide Fuel with an Inert Matrix and Burnup of About 19 % h.a. in BOR – 60*, 2011, Atomic Energy 109 (6), pp. 369 – 374
- [SAH 10] Saha, B., Acharya, J., Sands, T.D., Waghmare, U.V., *Electronic structure, phonons, and thermal properties of ScN, ZrN and HfN: A first-principles study*, 2010, Journal of Applied Physics 107 (3), art.no. 033715

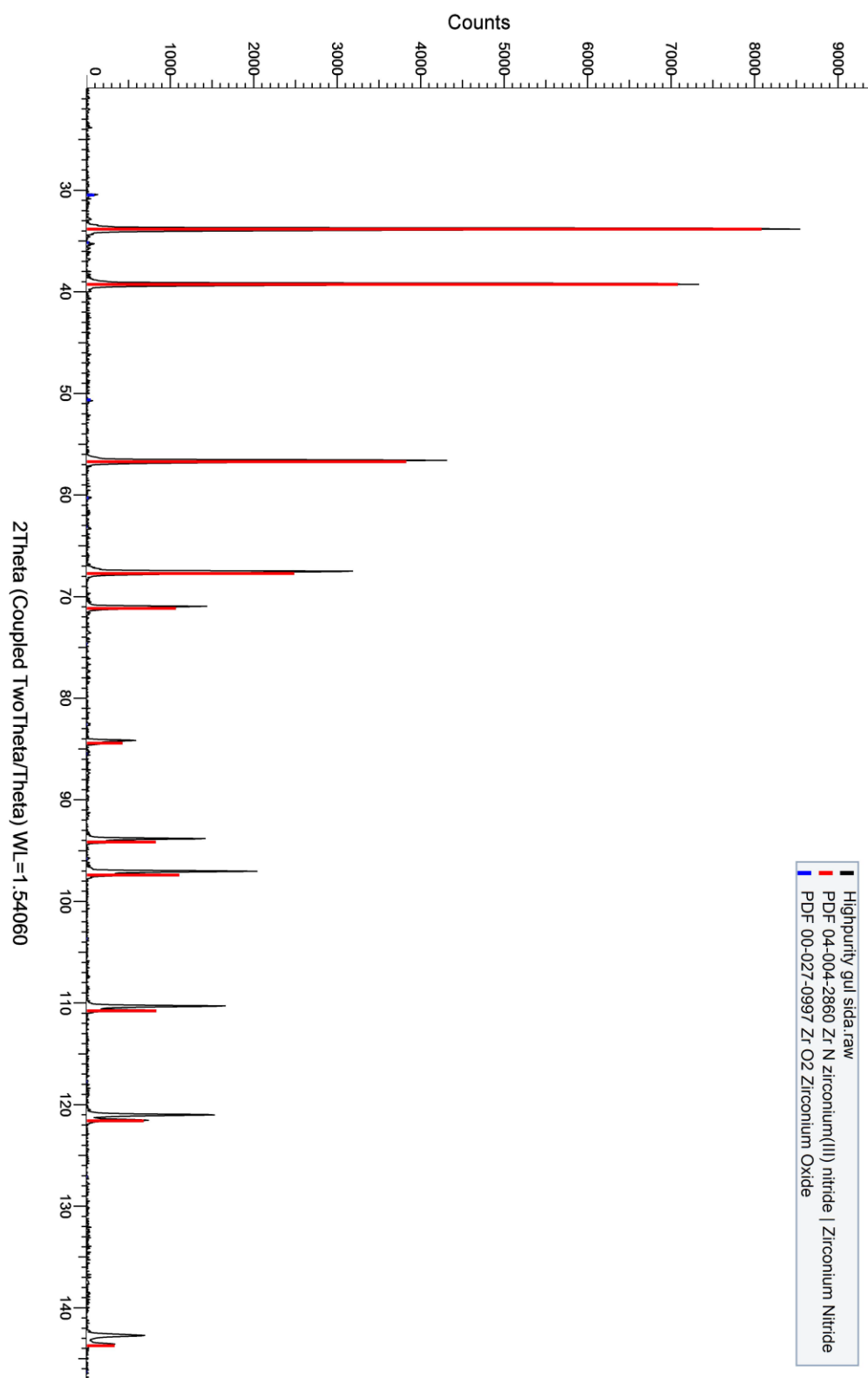
- [SHE 00] Sherif El - Eskandarany, M., Ashour, A.H., *Mechanically induced gas – solid reaction for the synthesis of nanocrystalline ZrN powders and their subsequent consolidations*, 2000, Journal of Alloys and Compounds 313, pp. 224 – 234
- [SMA 05] Smart, L.E., Moore, E.A., *Solid State Chemistry – An Introduction 3<sup>rd</sup> edition*, Boca Raton, Taylor & Francis, 2005
- [SOM 11] Somers, J., *Minor Actinide Bearing Fuels: Fabrication and Irradiation Experience in Europe*, 2011, Energy Procedia 7, pp. 169 – 176
- [STR 03] Streit, M., Ingold, F., Pouchon, M., Gauckler, L.J., Ottaviani, J.-P., *Zirconium nitride as inert matrix for fast systems*, 2003, Journal of Nuclear Materials 319, pp. 51-58
- [TAN 94] Tan, B.J., Xiao, Y., Galasso, F.S., Suib, S.L., *Thermodynamimc Analysis and Synthesis of Zirconium Nitride by Thermal Nitridation of Sol – Gel Zirconium Oxide*, 1994, Chemistry of Materials 6 (7), pp. 918 – 926
- [TSU 99] Tsukada, T., Venigalla, S., Morrone, A.A., Adair, J.H., *Low-Temperature Hydrothermal Synthesis of Yttrium-Doped Zirconia Powders*, 1999, Journal of the American Ceramic Society 82 (5), pp. 1169 - 1174
- [VAI 87] Vaidya, V.N., Mukerjee, S.K., Joshi, J.K., Kamat, R.V., Sood, D.D., *A study of chemical parameters of the internal gelation based Sol-Gel process for uranium dioxide*, 1987, Journal of Nuclear Materials 148, pp. 324 – 331
- [VAI 08] Vaidya, V.N., *Status of sol – gel process for nuclear fuel*, 2008, Journal of Sol-Gel science and Technology 46 (3), pp. 369 – 381
- [VĀL 14] Vālu, O.S., Beneš, O., Konings, R.J.M., Hein, H., *The high temperature heat capacity of the (Th, Pu)O<sub>2</sub> system*, 2014, Journal of Chemical Thermodynamics 68, pp. 122 – 127
- [VER 07] Verfondern, K., Nabielek, H., Kendall, J.M., *coated particle fuel for high temperature gas cooled reactors*, 2007, Nuclear Engineering and Technology 39 (5), pp. 603 – 616
- [WAL 09] Wallenius, J., Fokau, A., *A low power fast reactor cooled by natural circulation of LBE*, 2009, Proceedings from GLOBAL 2009 paper 9150, pp. 1669 – 1673
- [WAL 11] Wallenius, J., *Transmutation of Nuclear Waste*, Märsta, Leadcold books and games, 2011
- [WAL 12] Wallenius, J., Suvdantsetseg, E., Fokau, A., *ELECTRA: European Lead – Cooled Training Reactor*, 2012, Nuclear Technology 177, pp. 303 – 313
- [YEA 08] Yeamans, C.B., Chinthaka Silva, G.W., Cerefice, G.S., Czerwinski, K.R., Hartmann, T., Burrell, A.K., Sattelberger, A.P., *Oxidative ammonolysis of uranium(IV) fluorides to uranium(VI) nitride*, 2008, Journal of Nuclear Materials 374, pp. 75 – 78

## 10. List of abbreviations

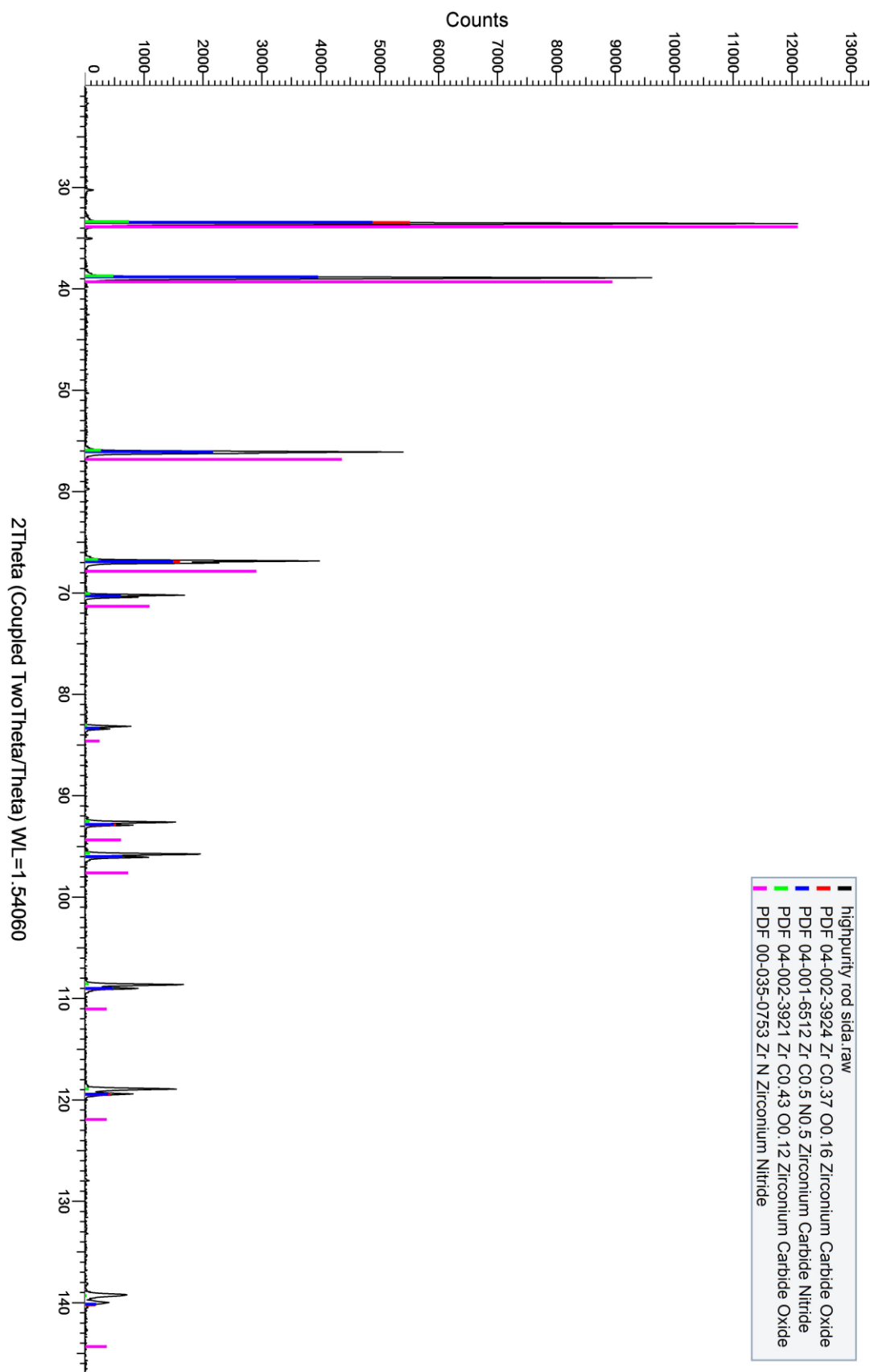
ADUN	<u>A</u> cid <u>D</u> eficient <u>U</u> ranyl <u>N</u> itrate
BWR	<u>B</u> oiling <u>W</u> ater <u>R</u> eactor
CNP	<u>C</u> arbon <u>N</u> ano <u>P</u> owder
CNT	<u>C</u> arbon <u>N</u> ano <u>T</u> ubes
DPA	<u>D</u> islocations <u>P</u> er <u>A</u> tom
EDX	<u>E</u> nergy <u>D</u> ispersive <u>X</u> -ray spectroscopy
HMTA	<u>H</u> exa <u>M</u> ethylene <u>T</u> etr <u>A</u> mine
IMF	<u>I</u> ncert <u>M</u> atrix <u>F</u> uel
LMFBR	<u>L</u> iquid <u>M</u> etal <u>F</u> ast <u>B</u> reeder <u>R</u> eactor
MOX	<u>M</u> ixed <u>O</u> Xide (fuel)
PCMI	<u>P</u> ellet <u>C</u> ladding <u>M</u> echanical <u>I</u> nteraction
PWR	<u>P</u> ressurized <u>W</u> ater <u>R</u> eactor
SEM	<u>S</u> canning <u>E</u> lectron <u>M</u> icroscopy
TD	<u>T</u> heoretical <u>D</u> ensity
XRD	<u>X</u> - <u>R</u> ay <u>D</u> iffraction
2EH	<u>2</u> - <u>E</u> thyl-1- <u>H</u> exanol

# Appendix I

ZrN sintered in high purity N<sub>2</sub>, “yellow side”



ZrN sintered in high purity N<sub>2</sub> “red side”



# ZrN sintered in high purity N2 “both sides”

